Interreg
EUROPEAN UNION
2 Seas Mers Zeeën
Polder2C's
European Regional Development Fund

Design and application of an overflow generator

Adaptation to climate change

Design and application of an overflow generator

Version:

20230424

Authors:

Vercruysse, J.; Depreiter, D.; López Castaño, S.; Verelst, K.; Peeters, P.

Ref.:

WL2023R20_047_1

This project has received funding from the Interreg 2 Seas programme 2014-2020 co-funded by the European Regional Development Fund under subsidy contract No [2S07-023]

Cover figure © INTERREG Polder2C's

Legal notice

Copyright and citation

D/2024/3241/299

This publication should be cited as follows:

Vercruysse, J.; Depreiter, D.; López Castaño, S.; Verelst, K.; Peeters, P. (2023). Design and application of an overflow generator. Version 4.0. FH Reports, 20_047_1. Flanders Hydraulics: Antwerp

Document identification

Customer:	Flanders Hydraulics	Ref.:	WL2023R20_047_1
Keywords (3-5):	Levee; Overflow, Field measurements, Overflow generator		
Knowledge domains:	Hydraulic structures > Dikes, shores and other flood defenses > erosion protection > in-situ measurements		
Text (p.):	46	Appendices (p.):	/
Confidential:	☒ No	☒ Available online	

Author(s):	Vercruysse, J. ; Depreiter, D.; López Castaño, S.

Control

	Name	Signature
Reviser(s):	Peeters, P.	Getekend door:Patrik Peeters (Signature) Getekend op:2025-01-06 16:37:57 +01:0 Reden:Ik keur dit document goed Peeters Patrik Vlaamse overheid
Project leader:	Verelst, K.	Getekend door:Kristof Verelst (Signature) Getekend op:2025-01-06 16:27:22 +01:0 Reden:Ik keur dit document goed Verelst Kristof Vlaamse overheid

Approval

Head of Division:	Bellafkih, K.	Getekend door:Abdelkarim Bellafkih (Sig Getekend op:2025-01-07 09:25:27 +01:0 Reden:Ik keur dit document goed Bellafkih Abdelkarim Vlaamse overheid

Table of contents

This project has received funding from the Interreg 2 Seas programme 2014-2020 co-funded by the European Regional Development Fund under subsidy contract No [2S07-023]

INTERREG Polder2C's project

The INTERREG Polder2C's is an international research project within the framework of the updated Sigmaplan for the river Schelde. The Hedwige-Prosperpolder will be transformed into tidal nature. Depoldering of Hedwige-Prosperpolder offers a unique testing ground, the Living Lab Hedwige-Prosperpolder, for flood defence and emergency response experts. In this environment current and innovative techniques, processes, methods and products can be tested for practical validation. Thirteen project partners, led by the Dutch Foundation of Applied Water Research (STOWA) and the Flemish Department of Mobility and Public Works (DMOW, Flanders Hydraulics Research), are working together. Together, they aim to improve the 2 Seas regions' capacity to adapt to the challenges caused by climate change.

Flood Defence

The rising sea level is a serious threat to the countries in 2 Seas region. How strong are our current flood defences? What is the impact of environmental elements such as the weather, the presence of vegetation or man-made objects on our flood defences? To answer these questions numerous destructive field tests are carried out in the Living Lab to validate flood defence practices. The project entails in situ testing, guidance on levee maintenance and validation of flood defence infrastructure.

Emergency Response

We aim to improve emergency response by developing the right tools for inspection of water defences, risk evaluation and solutions for flooding. If our water defences do not operate as designed, we must take the right measures to prevent flooding of valuable areas. The Hedwige-Prosperpolder Living Lab offers unique possibilities to exercise emergency management in the event of calamities under controlled but realistic circumstances. Activities that are part of the programme are levee surveillance and monitoring, emergency response exercises, breach initiation and the large European exercise.

Knowledge Infrastructure

We aim to develop a knowledge infrastructure through which existing and new to be developed knowledge will become available and accessible. A necessary success factor for any initiative to improve knowledge is to have its outcomes integrated in practices of a wider community. Knowledge Infrastructure focuses therefore on the consolidation of knowledge acquired in the Living Lab with a variety of activities. Accessibility of data in a user-friendly manner, educational activities in the field and incorporation of knowledge in educational curricula are considered key elements.

Field Station

How can we make sure that both experts in the field and the local public benefit from our project and the learnings about climate change, flood resilience, emergency response and the unique environment of the Hedwige-Prosperpolder? An important and unique way of reaching this goal is realising a Field Station at the project site. It will be used during and after the project for educational purposes, research and as a special meeting place for exclusive occasions.

This project has received funding from the Interreg 2 Seas programme 2014-2020 co-funded by the European Regional Development Fund under subsidy contract No [2S07-023]

1 Introduction

Overflow tests on levees are performed to gain insights in the strength of levees and levee covers under the load of continuously overflowing of water. Within the framework of the Poplder2C's project Flanders Hydraulics Research has designed and built a steady overflow generator, allowing to generate a controlled and homogenous discharge of water over the levee crest.

During both winters of 2020-2021 and 2021-2022, 25 overflow tests have been executed with this overflow generator on Belgian and Dutch levee stretches. The tests were carried out in 3 episodes from 30/10/20 to 28/11/20, from 17/02/21 to 31/03/21 and from 16/11/21 to 20/12/21. Different test goals have been addressed with focus on erosion resistance, to understand the performance of a levee cover (reference sections). Besides this also the influence of different anomalies and/or deviations from the 'standard' levee were investigated, including high-discharge alternative vegetation(reed, trees), anomalies of different types (burrows, slope anomalies),measures to protect or repair such anomalies (slope damage repairs, reinforced turf mats, burrow protection) and the erosion of the clay erosion layer. The results of these tests are described in a series of factual data reports and a summary report (see Annex A for a complete list).

The present report provides a description of the test setup and the validation of the overflow tests. The test setup includes the complete installation of a test section in the field and shows the different implemented monitoring activities The validation of measurements and discussion of the reliability is based on intercomparison of different sources. The report ends with suggestions regarding to monitoring during future overflow experiments.

This project has received funding from the Interreg 2 Seas programme 2014-2020 co-funded by the European Regional Development Fund under subsidy contract No [2S07-023]

2 Setup, calibration and preprocessing

2.1 General setup

During the Polder2C's project, tests were carried out for different purposes. For a detailed description of the different tests carried out is referred to the factual data reports ((Depreiter *et al.*, 2022c; b).

The **default** setup of a test strip consists of the following elements:

- A pump with water intake in a pool;
- Feeder system of metal or HDPE conduits between the pump and the overflow generator;
- The overflow generator;
- A test section containing several sensors and monitoring systems;
- A collection and recirculation trench to return the water to the intake pool.

An overview of the test set-up is presented in Figure 1. The overflow generator is positioned on the riverside of the levee just below crest level. From the overflow generator water is flowing over the crest towards the landward side of the levee slope. The water on the crest and the landward side of the levee slope is restricted by side boardings. On the crest and along slope different measurements are performed. The measurement equipment is mounted on portals. The individual measurements signals are transmitted to a data acquisition systems.

The discharge is foreseen by a local pump circuit. Water was pumped from a drainage trench at land side into tubes that running over the landward levee slope and the crest of the levee. On the crest of the levee the tubes run parallel with the crest towards the overflow generator. To test different sections the length of the supply tubes can be adjusted. Note that after overflow the water is captured in the drainage trench resulting into a closed system.

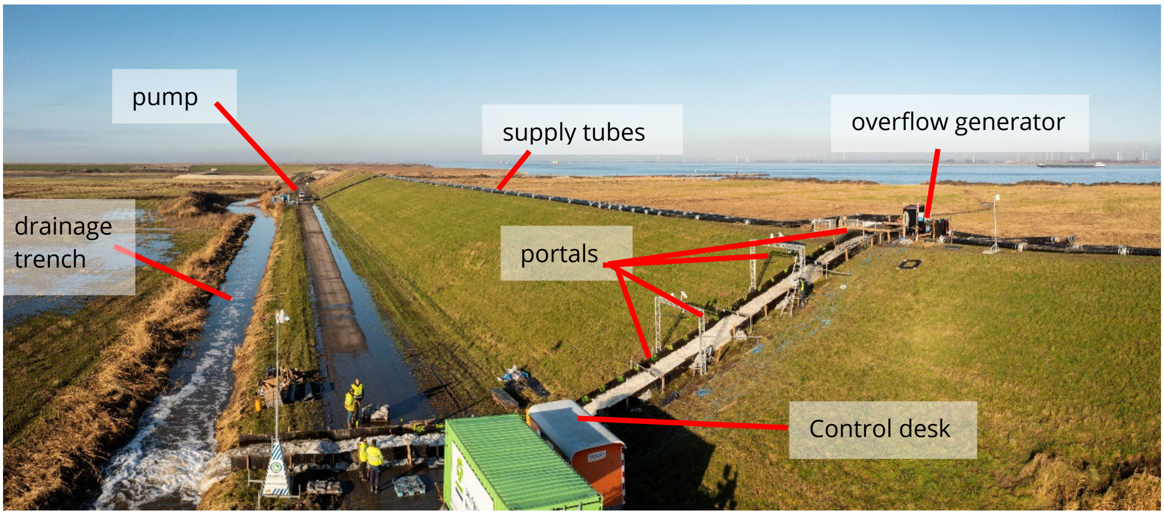

Figure 1 – General overview test set-up overflow tests

This project has received funding from the Interreg 2 Seas programme 2014-2020 co-funded by the European Regional Development Fund under subsidy contract No [2S07-023]

Discharge supply system

During each period of overflow experiments, different pump setups have been applied. During the winter 2020 experiments, a dual Hidrostal F10K dual pump setup (37 kW each) was supplied by Eekels BV. The pumps were driven by 150 kVA diesel power generators. A different, (single) pump setup was used in spring 2021 to higher discharges, using a Hidrostal I16K-HD (98 kW). The system was connected to metal DN500 (winter) and DN600 (spring) feeder tubes being directed towards the levee crest and being connected by a flange on the dissipation box of the overflow generator. The system with steel tubes proved to be not that flexible. It took quite some time to algin the tubes and bolt the flanges. After passing the crest the tube was lowered by means of elbows. No deaeration valve was foreseen at this point and it is assumed that air was trapped resulting in a reduction of the discharge. When repositioning the generator the inlet flange of the overflow generator needed to be exactly aligned with the tube. T

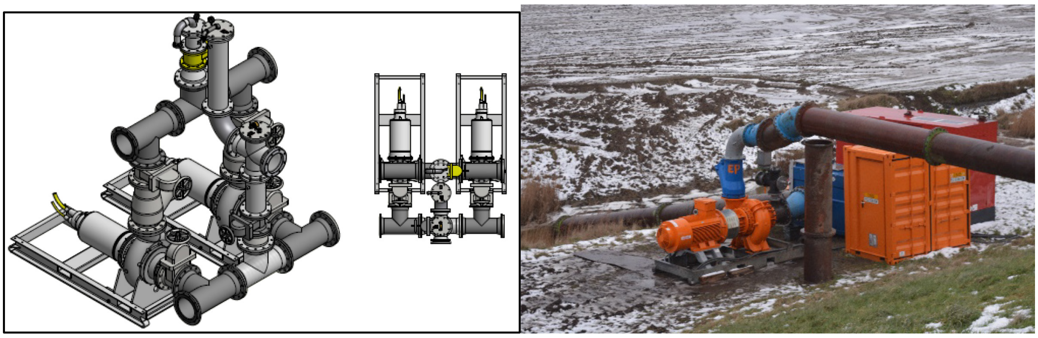

Figure 2 - Technical drawing (left) of the dual Hidrostal pump setup (winter 2020) and the single pump setup (spring 2021).

Figure 3 – Steel tube system right: pressurized entrance to dissipation box

During the winter 2021 period, two BBA pumps (BA300 and BA500) were supplied by Waterschap Brabantse Delta[1]. The pumps from Waterschap Brabantse Delta were submersible pumps in normal cases being used for emergency response. These pumps were coupled to 5 parallel HDPE feeder tubes. The feeder tubes were connected by clamps. It was not possible to connect the HDPE tubes to the inlet flange of the overflow generator. Therefore the outflow of the tubes were emitting by T-end connections directly onto the water surface of

[1] We hereby thanks the Waterschap Brabantse Delta for providing the pumping capacity during the third period of overflow tests. Highly appreciated!

This project has received funding from the Interreg 2 Seas programme 2014-2020 co-funded by the European Regional Development Fund under subsidy contract No [2S07-023]

the overflow generator (Figure 8). The system with parallel HDPE tubes proved to be much more flexible compared with the steel tubes used during the previous testing periods. Because the overflow generator was designed with a pressurized intake connected to a submerged dissipation box, the outflow out of the generator was disturbed during the last testing period.

Figure 4 – Setup with two individual BBA pumps and parallel feeder lines.

Overflow generator

The goal of the overflow generator is to dissipate the incoming discharge from the tube(s) into an evenly distributed subcritical flow towards the levee crest. The overflow generator was designed and developed by Flanders Hydraulics.

The design was performed in 3D CAD software. The chosen material was High Density Polyethylene (HDPE) plate material because of its design flexibility, price and material characteristics. An export of the CAD design drawing is presented in Figure 5. The different elements of the generator are indicated on Figure 6. For structural reasons stiffeners are welded on the HDPE plates, flanges are foreseen as well as a central beam. To be able to adapt the generator to the slope of the levee the generator consist of three separate elements connected by flanges. By adjusting the base element the generator could be optimized on the foreseen riverside levee slope. For the tests within the Polder2C's project, only 1 base element was developed. A main disadvantage of the current design is the absence of any means to correct for deviations in level of the overflow generator or deviations in the slope of the levee after positioning the generator. This resulted into the overflow generator being not always perfectly leveled. For a discussion of the impact, see Integration report (Depreiter *et al.*, 2022a).

This project has received funding from the Interreg 2 Seas programme 2014-2020 co-funded by the European Regional Development Fund under subsidy contract No [2S07-023]

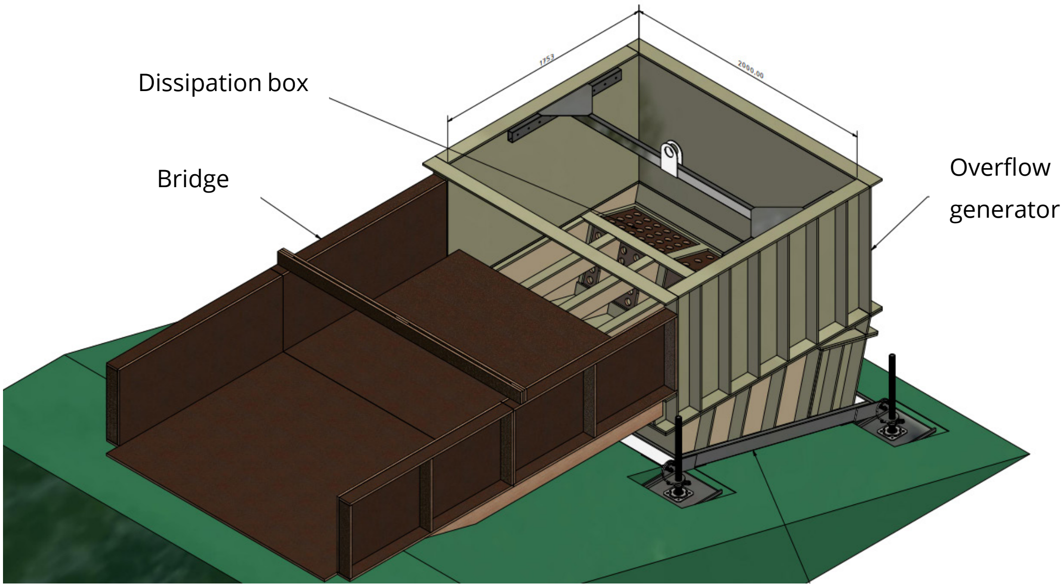

Figure 5 - Design drawing of the overflow generator.

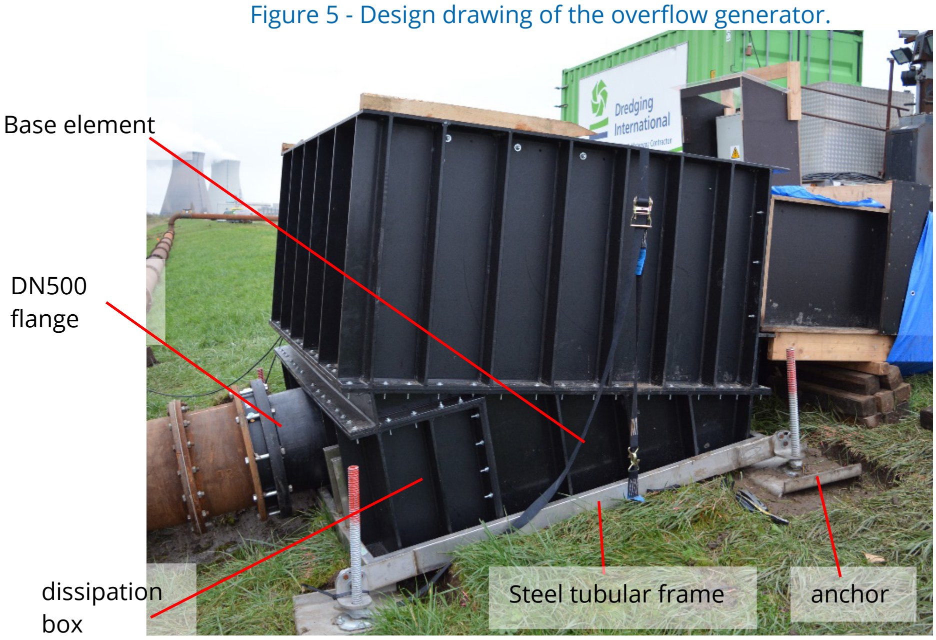

Figure 6 – Different elements of the overflow generator

The design maximum water discharge is 1 m^3/s which corresponds to approx. 0.50 m overflow above the levee crest. The discharge tube is connected by a DN500 flange to the generator. The inflow is dissipated in a rectangular dissipation box over the full width of the generator. The dissipation and spreading of the flow is regulated by perforated wooden plates (Figure 7, left). It was foreseen to optimize the perforated wooden plates before starting the tests but after the first run it was concluded that dissipation and spreading was already optimal.

This project has received funding from the Interreg 2 Seas programme 2014-2020 co-funded by the European Regional Development Fund under subsidy contract No [2S07-023]

Figure 7 – Dissipation box (left) and bridge (right)

The weight of the generator and the containing water mass is directly transferred by the bottom towards the levee surface. To keep the overflow generator in place, it is positioned onto a frame of steel tubular profiles, being fixed with anchors at the four corners of the frame. The anchors are positioned in local horizontal incisions (step) in the levee slope. During the first test, the steel tubular frame was levelled out, then the anchors were fixed followed by the placement of the overflow generator within the tubular frame. For the tests latter on the frame with the anchors was attached to the overflow generator, allowing to position the frame with the anchors by means of an excavator in one movement after creating the local incisions in the levee slope. The anchors where fixed to the levee slope after positioning.

A bridge made of plywood plate material with a support structure of wooden beams connects the overflow generator with the crest of the levee (see Figure 5 and Figure 7). The water tightness from the generator towards the crest is foreseen by an tarpaulin or an EPDM sheet.

During the third test period the overflow generator was fed by parallel HDPE tubes directly emerging into the water surface of the overflow generator resulting into a less optimal dissipation, see Figure 8. The latter system with HDPE tubes, however, proved to be much more flexible. For overflow tests to come were the generator is fed by a set of HDPE tubes emerging from the top, adapting the overflow generator should be considered. Note that during the design phase of the overflow generator also a setup with a tube emerging from the top into the overflow generator was considered. An ideal hydraulic design with a top inlet consists of a first chamber for the inlet of water from the back of the generator or from the top and a second chamber for the outflow. In between both chambers a separation must be provided. Dissipation can be foreseen by providing dissipation structures or by narrowing the slit in between both chambers and increasing the pressure. Because of the increased dimensions and the design risks, this design was not retained.

This project has received funding from the Interreg 2 Seas programme 2014-2020 co-funded by the European Regional Development Fund under subsidy contract No [2S07-023]

Figure 8 – Emitting of water from the supply tubes to the water surface during the third test period

Note that for the present design, it was difficult to place the generator at the correct level/height and to adapt the generator to the actual levee slope.. A new design of the overflow generator could include the outflow of the generator being positioned lower than the crest level, resulting into . an easier set-up and more realistic hydraulic conditions. As a consequence the height of the generator should be increased.

The chosen material for the generator, HDPE, proved to be optimal regarding design freedom, strength, flexibility, weight and durability. After the three test periods the HDPE generator is still in a good condition.

Test section with side boarding

From the end of the overflow generator bridge, along levee crest, landward side slope and toe until the drainage trench, side boardings were placed to construct a 2 m wide confined test section for water to flow.

For setting the side boardings, GPS points were staked out to ensure a flow direction perpendicular to the levee axis. Along the points, first paint was sprayed along a line using a mason’s rope. Then along this line, a small cut was made in the grass cover layer using a lawn edger for guiding side boardings when driven into the soil. Afterwards pointed wooden poles, having a length of 1.0 m and a cross section of 50 mm x 70 mm were hammered into the ground by means of a mechanical fence pole driver. The top section of the wooden pales was adjusted to a cross section of 50 mm x 50 mm to be able to use the mechanical pole driver. Concrete plywood plates with a length 2.44 m, a width 0.61 m and thickness 12 mm were used as side boardings. Subsequently, the 12 mm thick concrete plywood panels were driven into the ground (by hammering) until a depth of up to 15 cm. The panels were then screwed onto the poles. Both the side boarding and poles proved to be sufficient though not over dimensioned. At first, both placing of the side boards and the poles was done manually. From safety and also efficiency concerns this was not favourable and the lawn edger and a mechanical pole driver were implemented.

This project has received funding from the Interreg 2 Seas programme 2014-2020 co-funded by the European Regional Development Fund under subsidy contract No [2S07-023]

Figure 9 – Side boardings (left overflow tests, right: INFRAM overtopping tests)

To close the gap between the side boardings, the boardings were placed with some overlap in a fish bone pattern. An adjustment for tests to come, could be to place the side boardings without overlap and sealing the gapes by metal plates (Fig. 9 right, courtesy INFRAM).
During the overflow tests, local erosion near the boardings sometimes penetrated below the bottom of the side boardings resulting into spilling of water. The remediation consisted of driving the side boardings deeper into the ground and reinforcing the outside of the section with sand bags or tubes, see Figure 10. A complete avoidance of spillage was difficult to achieve. During the wave overtopping tests leakages where sealed by means of thin metallic plates placed at the flow section in front of the side boarding. For future overflow tests this should be considered. During some tests a plywood side boarding was replaced by a transparent (PMMA) side boarding to gain visual access to the flow within the test section (Figure 10 right).

Figure 10 –Leakages (left) and transparent side boarding (right)

Portals, sensors and (continuous) data acquisition

In order to monitor the hydraulic properties of the overflowing water and record the evolving damage, several sensors and observation systems have been installed over the test section. For this purpose, two types of portals were constructed. Three small portals (M1, M2, M3) to carry the ultrasonic water height sensors, the water measurement needles, and the electromagnetic flow velocity sensors. The two large portals carry cameras (C1, C2). Besides this default setup, additional sensors could be mounted on these portals, ad hoc. The large portals consisted of Light Truss profiles with a base formed by a solid rectangular plate. The

This project has received funding from the Interreg 2 Seas programme 2014-2020 co-funded by the European Regional Development Fund under subsidy contract No [2S07-023]

portals were quite heavy to handle, more specifically the base plate was heavy. The portals were not influenced by wind and it was possible to adjust the measurement set-up by placing a ladder against the portals. For future overflow tests it can be considered to use a lighter Light Truss profile without heavy base plate and to use tension strings instead of poles for bracing. Also the profiles used for the small portals were quite heavy. For the small portals and for the bracing of the large portals ground anchors were used, being installed and removed by means of a T-lever. This system proved to be efficient/effective. The default position of the sensors shown in Figure 11 is the theoretical case. In reality, there are (sometimes) deviations. Anyhow, most of the sections have been surveyed with RTK GPS and setup maps of the portals are provided in the factual data reports of each tests.

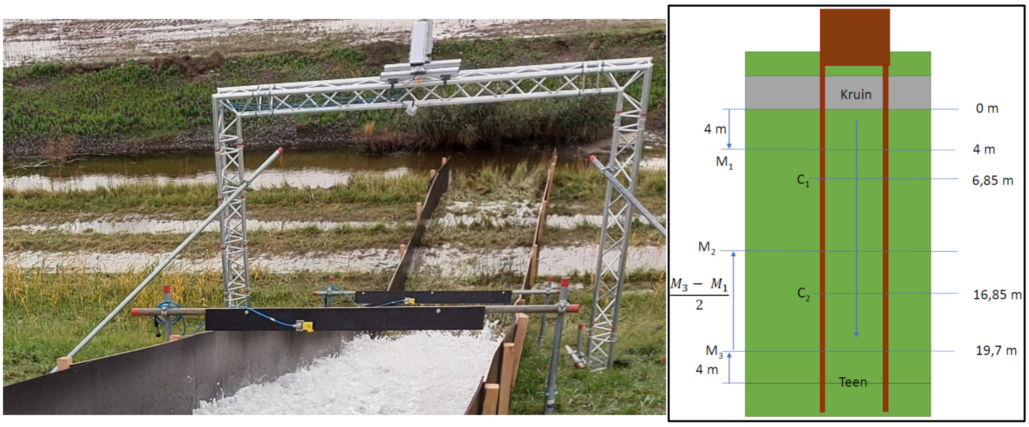

Figure 11 – Portals used for mounting equipment (left) and default positions sensors (right)

Data acquisition was performed on a data acquisition system (DAQ) designed and built by FH (AD conversion at 10 Hz). The discharge, point velocity and water height measurements generated a +/-10 V output signal. The measurement devices were connected by cables on to the side boarding of a cabinet containing the DAQ module, Figure 12 left. From the DAQ module the data was transferred by UTP to a control desk. The DAQ system and the camera recording system were running on two separate systems. The pulse for the camera system was controlled by the DAQ system, resulting into a synchronisation of the camera recordings with the DAQ system. Backup to the data servers at FH was executed overnight. For this purpose, a radio data transmission link was installed from the test site to a nearby site with ethernet availability.

To guarantee a clean power supply for the DAQ and the camera set-up as well as to prevent the risk of damage following power breaks, a set-up with a UPS powered by a dedicated generator was in place.

This project has received funding from the Interreg 2 Seas programme 2014-2020 co-funded by the European Regional Development Fund under subsidy contract No [2S07-023]

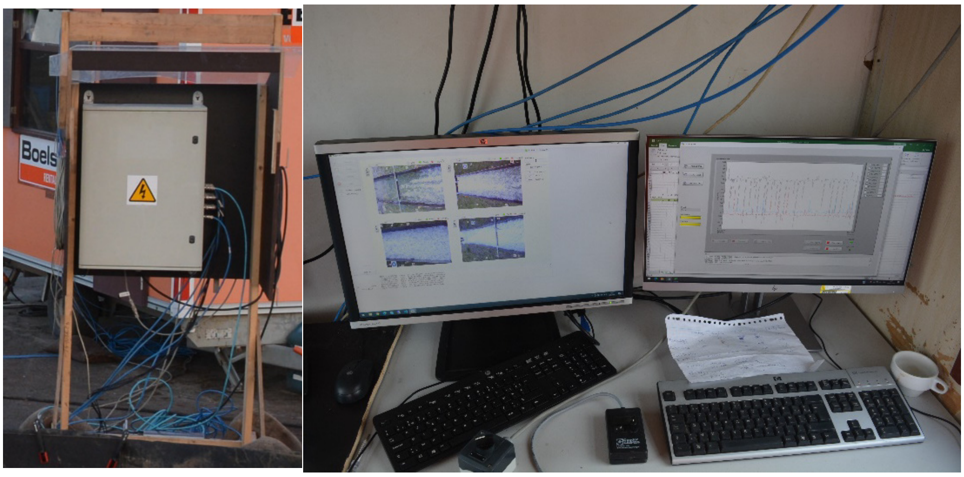

Figure 12 – Cabinet with DAQ modules (left), control desk (right)

During the tests, a logbook was kept to note test parameters, filenames, and notable events.

2.2 Cameras

Four industrial cameras type IDS uEye UI-5270SE-C-HQ with resolution 2056 x 1542 pixels where used. The cameras where connect to a computer using Ethernet cables , Figure 12. For reasons of simplicity only one computer was used, resulting into a framerate being limited to approx. 15 fps in a timespan of 20 s. This was sufficient for performing PTV velocity measurements.

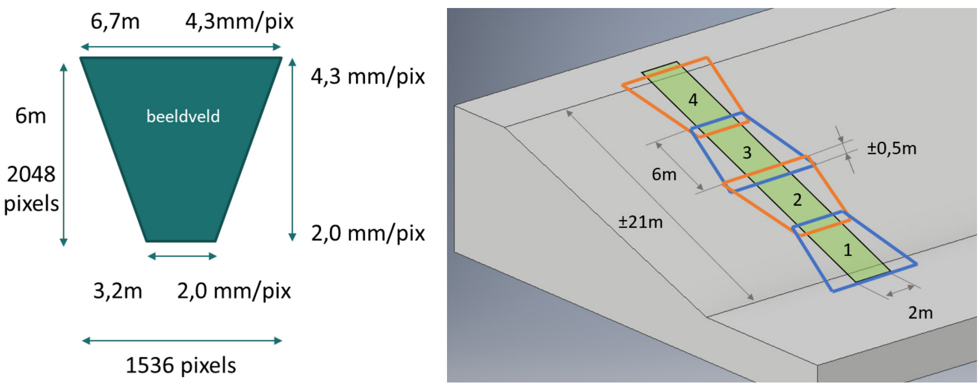

Figure 13 – Theoretical filed of view of the camera's (left) and levee coverage (right)

The 4 cameras were installed on the two camera portals. Each portal contained two cameras, the first was directed towards the crest of the levee, the other directed towards the toe of the levee. The resolution varies between 2.0 mm/pix directly under the portals till 4.3 mm/pix at a distance 6 m. For the purpose of merging and rectifying the images of the cameras, 28 photo markers were placed near the test section and their position was recorded using a RTK-GPS. Within the field of view of each camera, 6 markers where placed for merging the images and one additional marker with a grey scale was placed for colour and intensity rectification. The 6 reference markers used for rectification were placed symmetrical within the field of view of

 This project has received funding from the Interreg 2 Seas programme 2014-2020 co-funded by the European Regional Development Fund under subsidy contract No [2S07-023]

the camera. This was assessed as being sufficient. The markers with the grey scale were not used during the project and proved to be prone to reflection.

Control and acquisition of the cameras was managed from purpose-built software. Different camera profiles could be activated:

- "Surface picture": this camera profile was used totake images of the test section when no water is flowing. These images were taken to image the initial grass cover prior to the tests or to image the damage(d) state and were taken at a wide range of shutter times, providing that optimal lightened images were always available. Although not performed during the processing, creation of HDR images would be also be possible. The images where recorded in lossless compressed format ('.png).
- "Low frequent mode": ": Images are taken with an interval 5 minutes with burst of 8 pictures at a frequency of 2 Hz (other intervals may have been used) during flow conditions is captured, which can be used for observing the flow patterns. The images where recorded in lossless compressed format ('.png).The shutter time was set at automatic.
- "PTV mode": Pictures are taken during a short burst with high frequency (15 fps) for tracking a particle released one the crest. Due to data transfer rate the recording was done in an uncompressed format('.bmp'). The shutter time was set at automatic.

Note that these recordings resulted in a vast amount of data. The image size of one uncompressed image was 9Mb. The data-reduction when using a lossless compressed png format was limited (9Mb → 7 Mb). A typical surface picture resulted in approx. 200 Mb, a low frequent recording resulted in approx. 3 GB and a PTV measurement resulted in near 10 GB of data. For the surface picture, a fixed range of shutters times were used not taking into account the specific light conditions resulting in a set of over under- as well as overexposed recordings. For the low-frequency mode the concept of bursts is still believed to be valid, but the amount of images within one burst can be reduced from 8 till 3 or 4. During the design phase more hydraulic variation during the tests was expected. In hindsight, the hydraulic variation during one test proved to be, most of the times, negligible. For a next test program, a reduction immediately after the tests could be considered. This way the over- and underexposed images of the "Surface picture" profile could be already deleted For the "Low frequent" mode the time interval of 5 minutes can be kept or even reduced. If at the end of a test no significant damage or discharge variations has occurred, the data could be reduced to e.g. one burst every 20 minutes.

This project has received funding from the Interreg 2 Seas programme 2014-2020 co-funded by the European Regional Development Fund under subsidy contract No [2S07-023]

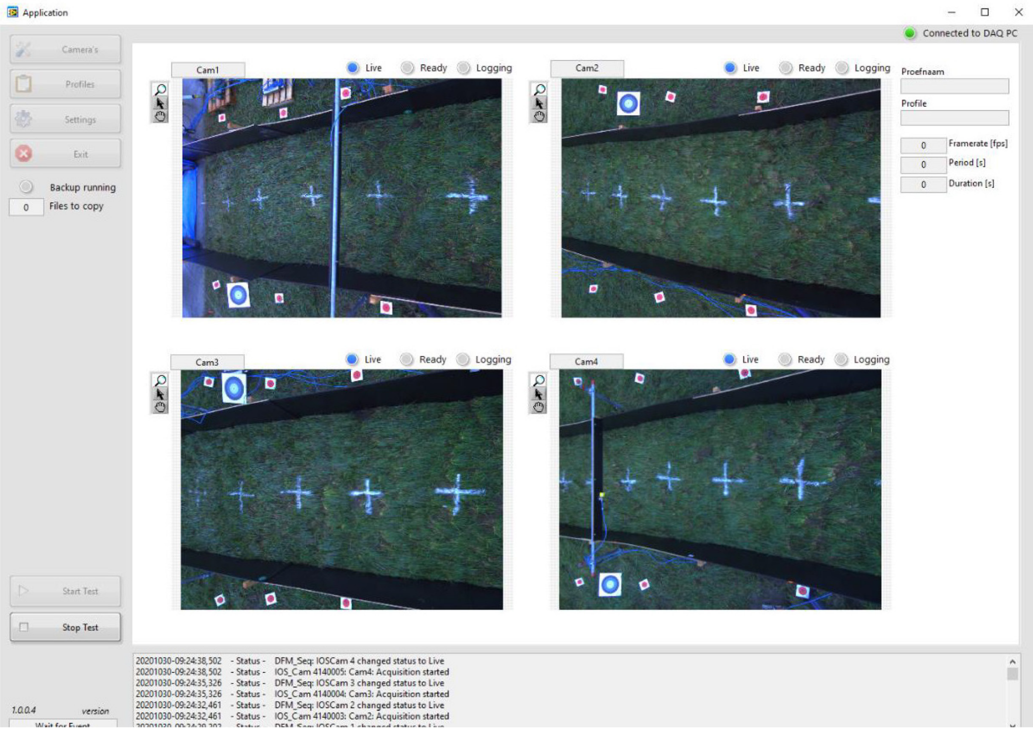

Figure 14 - Camera control software screenshot. Outside the test section, reference markers can be identified.

The presence of the reference markers allows to project the four images into one orthogonalized image. This was done with the use of the Skimage library in Python. First the XYZ-coordinates of the markers were projected onto one plane. To perform the projection four markers are sufficient. For control and back-up concerns two additional markers were used.

During design phase a set-up with different camera's on a vertical pole located at the toe of the levee was considered. In this set-up it was not possible to adjust angle, diaphragm and sharpness of the camera when in position. It was also feared that the image quality would be not sufficient. For the chosen set-up with four camera's the image resolution was optimized and all four camera's record the same, distorted, image.

Additional recordings were made using a IDS uEye UI-3060CP C UBS 3.0 camera with a maximum framerate of 166 fps and using a Krontech Chronos 2.1 Full HD high speed camera. Due to the maximum cable length of 5 m for a USB3 camera and the sensitivity and complexity of the Cronos high speed camera this measurements were only performed on some selected test sections. The goal of this additional measurements was validating the electromagnetic point velocity measurements and gaining additional insights in the hydraulics during overflow. The measurement of the water surface with the USB3 camera proved to be successful. For recording the water through the transparent side boarding the max. framerate of the USB3 camera (166 fps) proved to be insufficient. Since the Chronos high speed camera is a delicate device and the camera needed to be positioned just above the ground near the side boarding, the device was placed in a closed PMMA housing. Because of battery problems and working with the Chronos in muddy outdoor conditions proved to be challenging, the outcomes of these recordings were less promising than expected.

This project has received funding from the Interreg 2 Seas programme 2014-2020 co-funded by the European Regional Development Fund under subsidy contract No [2S07-023]

2.3 Discharge

The measurement of the input discharge has been performed using a Khrone Optisonic 6000 sensor with UFC300 transmitter. The sensor was installed on the steel tube on a flat (horizontal) part of the feeder pipe system.

Figure 15 – Set-up Khrone Optisonic discharge measurment

The Khrone Optisonic emits an ultrasonic signal through the tube shell, via the medium and again through the tube shell were it is registered. The measurement is very sensitive to the quality of the transmission of the ultrasonic wave. Before installation, the connection points on the tube wall were cleaned by a grinder and a special transmitting paste was used. The required characteristics of the pipe (material, wall thickness, diameter) were specified with care. The sensor was placed in a straight horizontal stretch but not at the highest position, because of the risk of entrapped air. On the tube the sensor was placed at 45° angle with respect to the horizontal as prescribed. To ensure a correct positioning of both sensors a frame was used. To prevent contamination of the signal by the pump frequency drive, the discharge measurement was powered by the UPS from the DAQ system. At a given point it was noticed that the cable to control the pump RPM was contaminating the DAQ system. This was solved by installing an electrical separator. Although the installation was handled with care by a specialist, the discharge measurement showed to be very sensitive for disturbances.
During the third test period, the setup with the BA pumps did not allow a direct control of the discharge through a frequency regulator but the pump power could be regulated to maintain a power (in rpm's) as required. Simultaneously, the discharge measurement often didn't work. To overcome total uncertainty, a RPM-discharge curve was set up. This relationship depends on the inlet water level, the outflow level and the hydraulic losses (which varied with different tube lengths).Therefore this relationship is not that accurate.
The relationship was determined during test N-OF04 for pump BA500 (Figure 16) and based on 3 different pump RPM's (1200 rpm, 1400 rpm and 1600 rpm), leading to the relation Q (L/s) = 372 + (RPM – 1200)*0.732.
A new calibration was performed during N-OF02, yielding more points and for both pumps (Figure 17):

- BA300: 87.4 + 0.598 x (RPM-1000) l/s
- BA500: 319.8 + 1.130 x (RPM-1200) l/s

This project has received funding from the Interreg 2 Seas programme 2014-2020 co-funded by the European Regional Development Fund under subsidy contract No [2S07-023]

The differences in BA500 relation between N-OF04 and N-OF02 may be due to differences in water head in the intake channel and conduit line length.
Apart from the observed discharge, for each test always a target discharge was defined. This target discharge is referred to as the nominal discharge of the experiment.

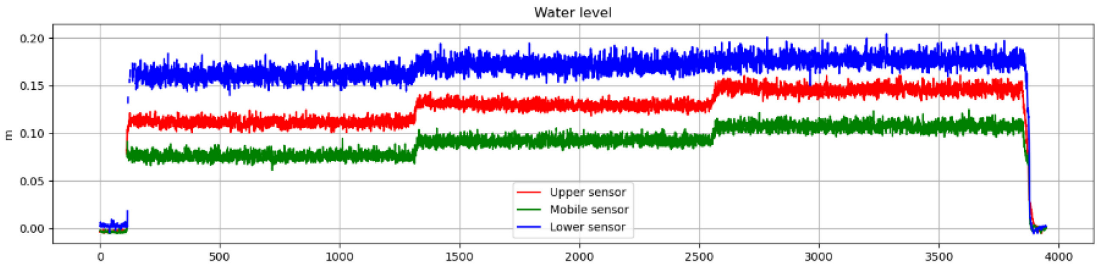

Figure 16 – Water height timeseries on which the RPM-Q relation for the BA500 pump was determined (Q measured with handheld monitor).

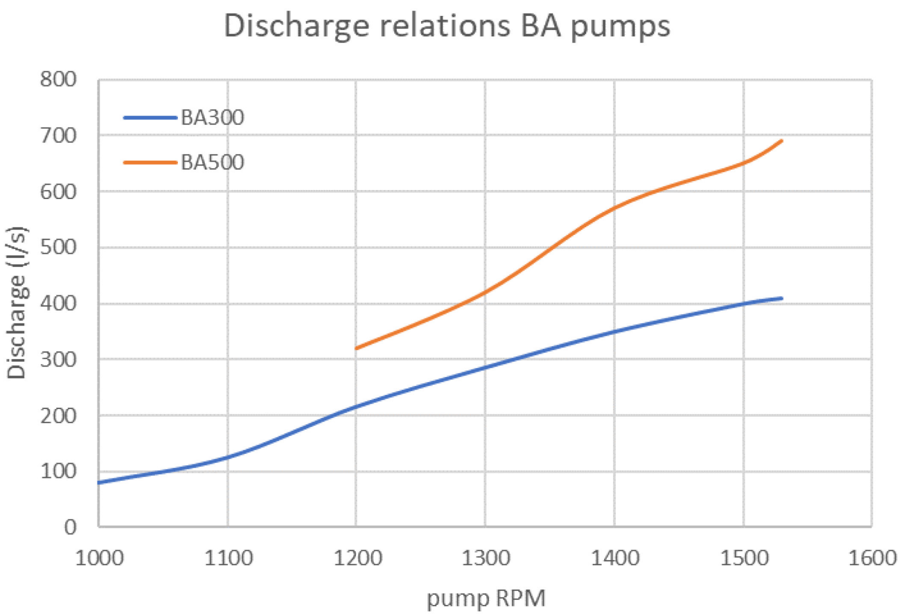

Figure 17 – Pump power vs discharge relations for the BA pumps used in winter '21.

The processing of the discharge timeseries consisted of the following steps:

1) De-spiking in order to remove the largest spikes. Only the largest spikes were removed, corresponding to data points being outside the 5-sigma window of the residuals after subtracting a bandpass-smoothed signal.
2) Executing a smoothing of the data set using a moving average with a window of 1 second using a uniform convolution filter.
3) Validation of the measured data. This is discussed later on in the report

The minimum validation that was carried out consisted of the calculation of the discharge at the crest level of the levee based on velocity and water height measurements. During experiment B-OF-03 a velocity sensor was placed on the crest. During flow block B6 of this

This project has received funding from the Interreg 2 Seas programme 2014-2020 co-funded by the European Regional Development Fund under subsidy contract No [2S07-023]

experiment, the average velocity and water height were recorded as 1.64 m/s and 22 cm. Manual water level measurements (with a ruler) yielded an average of 20.7 cm water height. Because this section was a 1 m wide section, the extrapolated discharge would be Q = A x h x V = 0.361 m^3/s or = 0.339 m^3/s depending on the water level used. The average discharge measured by the DAQ yielded a discharge of 0.337 m^3/s, which differs up to 7 % with the calculated values.

2.4 Water level

Default water level measurements were executed using ultrasonic Banner Engineering Q45ULIU64ACRQ6 sensors being installed at 4 small portals. The portals were situated at the crest and the locations M1, M2 and M3 corresponding to UPPER, MOBILE and LOWER positions on the slope). The exact position varies per test zone, but in general the following applies:

- The CREST sensor is positioned at the crest of the levee.
- On the levee itself, the UPPER sensor is positioned at about 1/4th of the slope length away from the slope break.
- The MOBILE sensor is positioned typically halfway the levee slope.
- The LOWER sensor is situated at approsimateley about 1/4th from the lower slope break were the slope transitions into the levee toe.

Figure 18 – Ultrasonic water level and electromagnetic point velocity meter mounted on small upper portal

The processing of the (raw) water level timeseries aimed at obtaining a reliable mean value. The processing of the water level timeseries therefore consisted of the following steps:

1) Recalibration of each timeseries, by re-adjusting the zero level based on the data recorded at the start or end of a block when discharge is not yet started or stopped. Note that this corresponds to an adjustment of the intercept of the calibration curve. Prior to the measurements the range was set in the lab and the slope of the calibration curve followed from a calibration over the selected range.
2) Despiking in order to remove the largest spikes (only the largest spikes were removed, corresponding to data points laying outside the 5-sigma window of the residuals after subtracting a bandpass-smoothed signal).
3) De-spiking in order to remove the largest spikes. Only the largest spikes were removed, corresponding to data points being outside the 5-sigma window of the residuals after subtracting a bandpass-smoothed signal.
4) Executing a smoothing of the data set using a moving average with a window of 1 second using a uniform convolution filter.

This project has received funding from the Interreg 2 Seas programme 2014-2020 co-funded by the European Regional Development Fund under subsidy contract No [2S07-023]

5) Validation of the measured data is discussed further in this report.

Other water level measurements have been carried out on selected test sections and at discrete times. These measurements include the use of rulers, which served as a check of the water level on the crest and which were noted in the logbook) and the use of a 2D line LiDAR scanner (see paragraph 2.8).
Concerning these ultrasonic water level measurements, the following uncertainties are noted. The actual water level is easily determined at the crest, but is more irregular and foaming at other sensor locations. Additionally, the crest of a dike is not perfectly flat. Theoretically, the water level should be measured on the highest point of a crest that is levelled over the width, these conditions are not met at all times, introducing an extra uncertainty on the measured water level.

2.5 Velocity

Standard point measurement of the flow velocity were executed by using up to three Valeport's Model 802 electromagnetic flow meters. This Valeport flow meter measures velocity in longitudinal and transversal direction separately. These flow meters were also used by INRAE to measure velocities on a slope during their overflow experiments on a lime threated levee in Southern France (Bonelli *et al.*, 2018). Note that INRAE modified the flow meters to be able to measure velocities exceeding 5 m/s. The flow meters were installed on the UPPER, MOBILE and LOWER position. Sometimes, the flow meters were placed at different positions (e.g. at the CREST portal). Such modifications of the test program are recorded in the logbook.

The velocity sensors were positioned so that the measurement point was situated between 2 and 5 cm above the bottom of the test section. However, the irregularity of the soil, the presence of vegetation patches, the evolution of both vegetation and soil during the test, and the possibility that detached vegetation get stuck on the sensor are all factors that contribute to uncertainty, noise and/or unwanted trends in the data that cannot be identified or isolated.

The processing of the velocity timeseries was aimed at obtaining a reliable mean velocity signal. The processing of the velocity timeseries therefore consisted of following steps:

1) Calculation of the velocity magnitude from the X and Y component of the measured velocity.
2) Despiking in order to remove the largest spikes (only the largest spikes were removed, corresponding to data points laying outside the 5-sigma window of the residuals after subtracting a bandpass-smoothed signal).
3) De-spiking in order to remove the largest spikes. Only the largest spikes were removed, corresponding to data points being outside the 5-sigma window of the residuals after subtracting a bandpass-smoothed signal.
4) Validation of the measured data is discussed further in this report.

Alternative velocity measurements have been performed on a selected test sections (and not continuously), consisting of LSPIV and PTV measurements (see § 2.6 and § 2.7).

This project has received funding from the Interreg 2 Seas programme 2014-2020 co-funded by the European Regional Development Fund under subsidy contract No [2S07-023]

2.6 LSPIV measurements

For LSPIV-measurements of the surface velocity an IDS UEye UI-3060CP-C-HQ USB3 camera was used. The main disadvantage of this USB3 camera is that the cable length is limited to 5 m. Therefore recordings were controlled on a laptop next to the model section and they could not be synchronized with the DAQ system. The maximum framerate of the USB3 camera is 166 fps. Due to some problems with the quality of the USB connection and the recording software the framerate was sometimes limited to 120 fps. The camera was mounted in between the large camera portals and was pointing perpendicular to the levee slope. For image transformation, a 1 m x 1 m reference frame was recorded before or after the test, see Figure 18. Based on the reference point an orthogonalization was applied on the images. In the resulting images the size of the pixels equals 1mm x 1 mm. For the transformation again the Skimage package was used in Python.

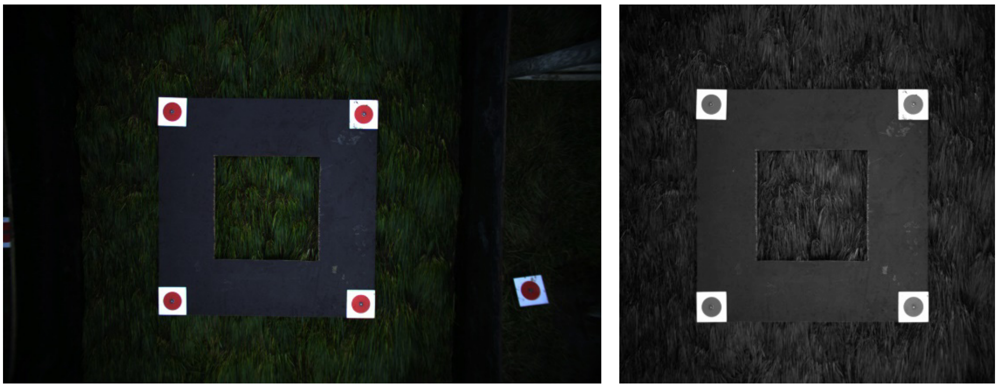

Figure 19 – Orthogonalization of image

After this transformation, the images were processed using the OpenPIV package version 0.24.0. A simplified filter was applied: consisting of filtering velocities that differ more than 50% from the mean velocity of the field and filtering velocities were the magnitude in y direction is greater than 20 % of the velocity in x direction.. An example of a processed LSPIV measurement step is presented in Figure 19.

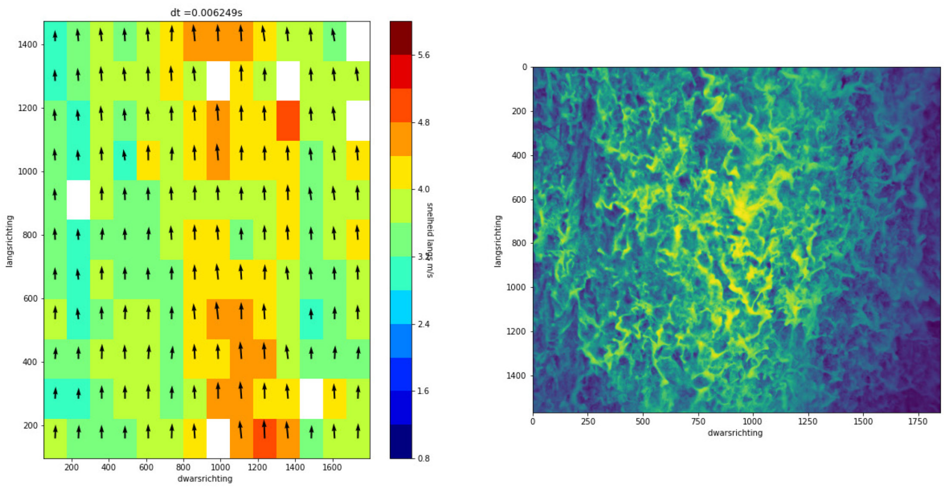

Figure 20 – Example Openpiv processing surface velocity (OF11 block11 Q3_160Hz_G0_E0.7**)**

This project has received funding from the Interreg 2 Seas programme 2014-2020 co-funded by the European Regional Development Fund under subsidy contract No [2S07-023]

2.7 Patricle tracking velocity measurements

For performing the particle tracking velocimetry (PTV)-measurements, a set-up with the 4 camera's for capturing overall images of flow and erosion is used. This setup was described in §2.2. The framerate was set to the maximum, i.e. 15 fps. The recording time was limited to 20 s. After this period of 20 s the RAM memory was filled and images dropped out. Immediately after the start of the PTV recording a floater was released at the crest. Both Ping-Pong as tennis ball were used as floater. The PTV was performed on the orthogonalized and merged image. For the orthogonalization one reference plane was created through the GPS locations of the reference marker. Note that at the crest and toe of the levee the slope differs from the remaining part of the levee, resulting into a deviation with respect to the reference plane. A second deviation occurs when the displacement of the particle is calculated based on two different source images. The floater, an orange Ping-Pong ball or red/yellow tennis ball, was tracked manually on the merged image. Due to the difference in illumination, the change in flow pattern when the flow gets aerated, the presence of red reference markers next to the test zone, and the floater that is drowned at certain moments, it was decided that manual tracking of the floater was the most efficient and accurate approach. By making use of Pyton and specific the OpenCV library the processing of one measurement proved to be in the order of minutes.

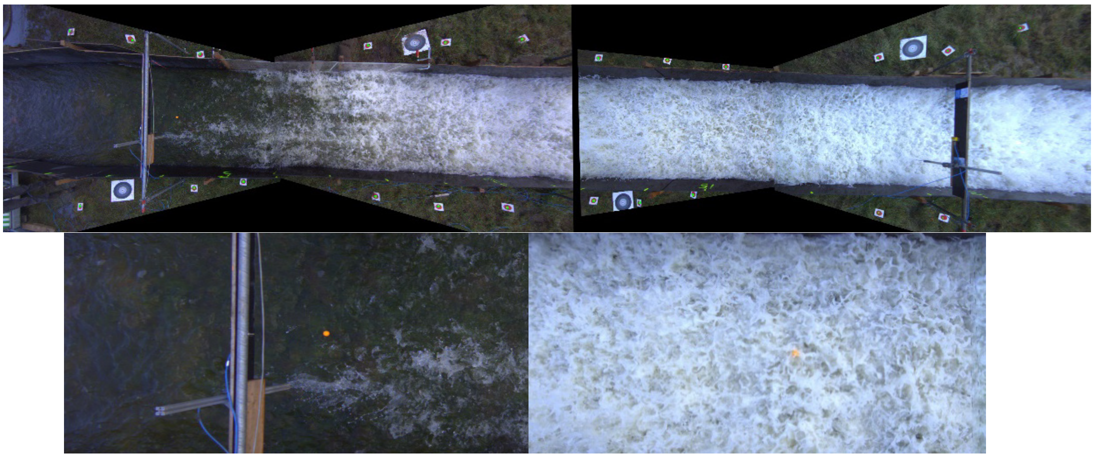

Figure 21 – Example PTV measurement (top merged image, lower particle) B-OF8-B8

2.8 Line LiDAR Scanner

On some selected sections, the Sick LMS511-20100 Pro line LiDAR scanner has been deployed. The LMS511 is a 2DLiDAR line scan, which means that the LIDAR rotates and measures the distance and the angle to the measurement instrument. For each scanline, a set of distances is acquired at different angle positions. Together, this generates a 'point cloud' at each angle position. Finally, a longitudinal or transversal elevation transect is obtained of either the ground surface or the water surface. The measurements are used in data comparison and validation further on in this report (§3.2; also the processing of the LiDAR data is described in this paragraph).

 This project has received funding from the Interreg 2 Seas programme 2014-2020 co-funded by the European Regional Development Fund under subsidy contract No [2S07-023]

For the measurements the scanner was mounted onto the sameportalsused for the recordings of the flow and the damage); these portals were positioned at approximately 1/3rd and 2/3rd of the slope length.. The scanner was aligned by means of a beam with indicator leds.

Figure 22 LiDAR and USB3 camera positioned on camera portal (left)
LiDAR beam indicator (right)

2.9 Topographic measurements

Different types of topographic measurements were performed.
For a general overview of the levee and outlining of the test section the available DEM was used: the Digital Terrain Model II (DHM2) for Flanders and the Digital elevation Model (AHN) for the Netherlands.
Besides this, a photogrammetry based DTM was derived from images shot with a drone in June 2022. The dataset encompassed the levee, but not the adjacent polders or marsh. This dataset yielded the T0 topographic measurement for the levee test site. These data sets are both available in meshed format as in a point cloud data format and proved to be very useable to derive the levee elevation, slope and large scale regularity.
Detailed measurements for example of deformation and erosion due to overflow were measured by a terrestrial LiDAR. Also a comparison between a professional terrestrial LiDAR and an Apple iPhone 12 Pro® (combining lidar and photogrammetry) (Depreiter *et al.*, 2022d) was performed. When working with well-known reference points the iPhone proved to be usable for characterizing small scale damages. For new overflow tests a handheld system (such as the iPhone Pro) with LiDAR or Time-of-Flight sensors, if used correctly, can be a nice tool to follow up erosion of a specific area with a smaller scale over time.
An RTK GPS was used to set-out the overflow sections and to register the positions of the reference markers and portals.

This project has received funding from the Interreg 2 Seas programme 2014-2020 co-funded by the European Regional Development Fund under subsidy contract No [2S07-023]

3 Validation

This chapter deals with the validation of the measurement set-up, more specific the water level and flow velocity measurements. The validation of the discharge meter is described in paragraph 2.3. During some tests, additional water level and velocity measurements were performed. The tests with additional measurements used for validation are described in §3.1. The validation of the water level sensors is addressed in §3.2 and the validation of the point velocity measurements is discussed in §3.3.

3.1 Test sections B-OF8, B-OF10, B-OF11 and N-OF03

The validation consists of the comparison followed by a discussion of data measurements from different sources. Depending on the instruments applied, different test sections are selected for validation. Within each test section, experiments are executed in blocks of typically 1 to 2 hour during which overflow is taking place. These blocks are numbered and referred to as such in the descriptions that follow.

The comparison and discussion was performed for the following five blocks:

- Section B-OF08 block 11 when additional measurements with LiDAR and PTV were executed,
- Section B-OF10 block 11 when additional measurements with LiDAR were executed,
- Section B-OF11 block 11 when additional LiDAR and LSPIV measurement equipment was positioned on the first camera portal.
- Section B-OF11 block 12 when additional LiDAR and LSPIV measurement equipment was positioned on the second camera portal.
- Section N-OF03 block 6 when additional measurements with the LiDAR were carried out.

These specific blocks are selected for the analysis because the discharge was varied within the course of these blocks. This allows not only to compare a 'static' velocity or water level, but allows to apply a relation between these parameters and the discharge applied, given insights about the accuracy.

A plot of the varying discharge for these five blocks is presented in Figure 22. Block N-OF03 is missing due to an malfunctioning discharge measurement. The test blocks are split up in sub blocks with constant discharge. The start of these blocks is indicated by dotted lines and the end by solid lines.

 This project has received funding from the Interreg 2 Seas programme 2014-2020 co-funded by the European Regional Development Fund under subsidy contract No [2S07-023]

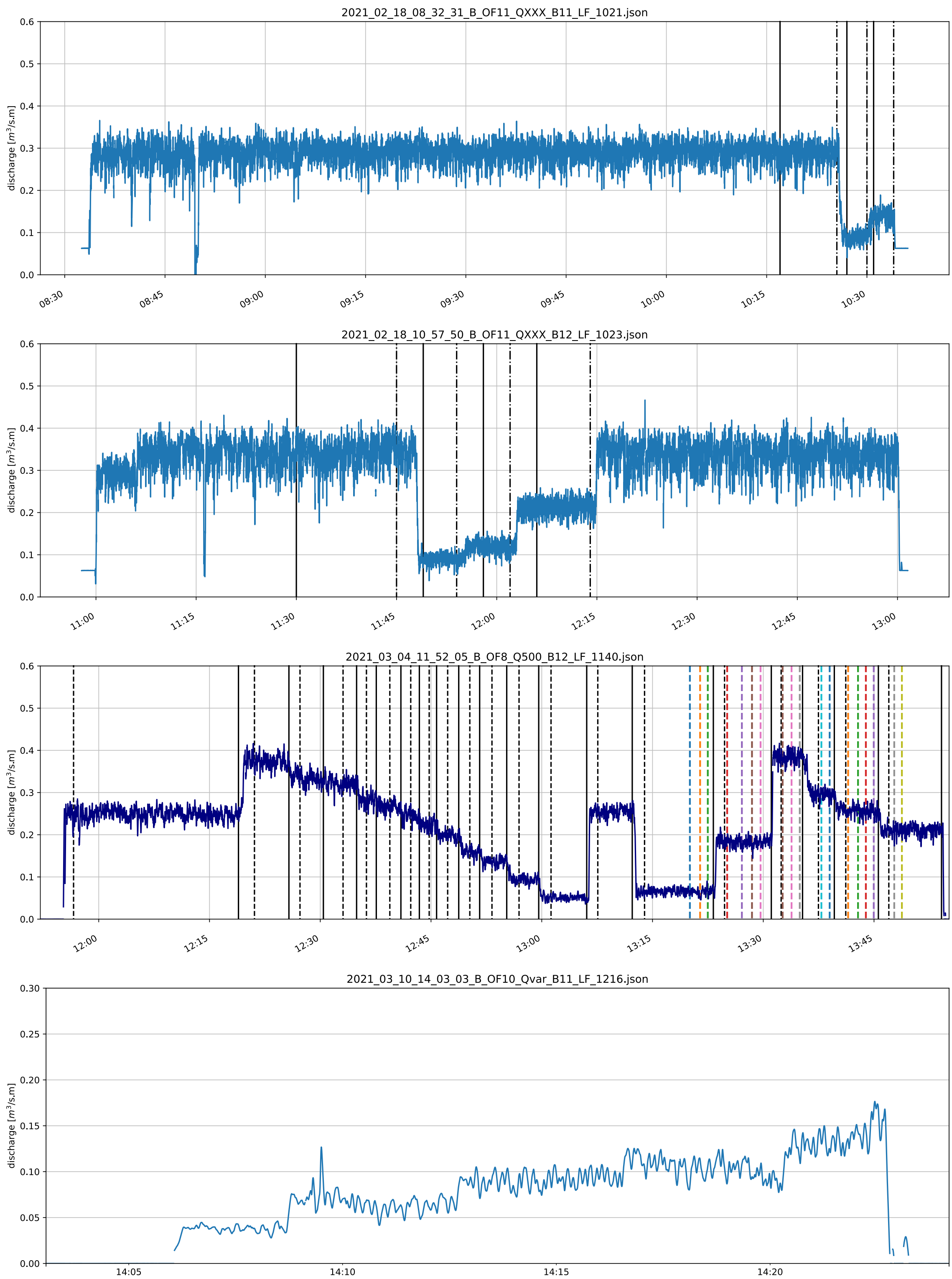

Figure 23 – Variation of discharge in time for the blocks selected for validation (top to bottom: B-OF11 Block 11; B-OF11 Block 12; B-OF08 Block 12 and B-OF10 Block 11).

Note that for B-OF8 block 12 there is also a variation in discharge during the first part of the block. The logbook noted that PIV measurements were performed, but unfortunately the data is missing.
The position of the portals and the sensors during the 5 blocks is presented in Figure 23.

This project has received funding from the Interreg 2 Seas programme 2014-2020 co-funded by the European Regional Development Fund under subsidy contract No [2S07-023]

Figure 24 - Position of sensors and portals during B-OF08 (left), B-OF10, B-OF11 and N-OF03 (right) - WH=water height sensor, VEL=point velocity meter, C= control point

3.2 Water height sensors

3.2.1 Methods

At a small number of tests, a 2D LiDAR line scanner (Sick LMS511-20100 Pro) has been used to scan the water surface.The water height data obtained from the ultrasonic sensors and the 2D LiDAR scanner are compared for a number of these tests. For more information on the methods, see §2.4 and §2.8. The measurements used for comparison are presented in §3.2.2, the intercomparison is given in §3.2.3, conclusions are formulated in §3.2.4.

3.2.2 Data and processing

Ultrasonic

The ultrasonic water height sensor data has been processed according to the description in §2.4. For tests with the discharge varying in time, subsections of the measurement blocks have been selected to calculate statistics.

LiDAR

A first step in processing is to average this point cloud into a single line as a function of the angle, shown in Figure 24. Note that the variation of the measured distance (between the scanhead and the detected object) during overflow shows a much larger variability compared to a measurement of the slope itself, i.e. without water flowing along the slope (compare Figure 24 and Figure 25). This is not the case for the fixed objects (the portals). The section shown in Figure 25 depicts a 750 L/s discharge situation, which is characterized by a strong foaming and spray.

As a next step, the scanline is converted from a polar to a cartesian system. Because the LiDAR scan head is not aimed horizontally but rather perpendicular to the levee slope, the cartesian projection of the geometry will not be correct. Therefore, we cannot speak of horizontal or vertical, but rather of parallel distance and orthogonal distance (with regard to the LiDAR tilt). This effect will be compensated for in a later step.

 This project has received funding from the Interreg 2 Seas programme 2014-2020 co-funded by the European Regional Development Fund under subsidy contract No [2S07-023]

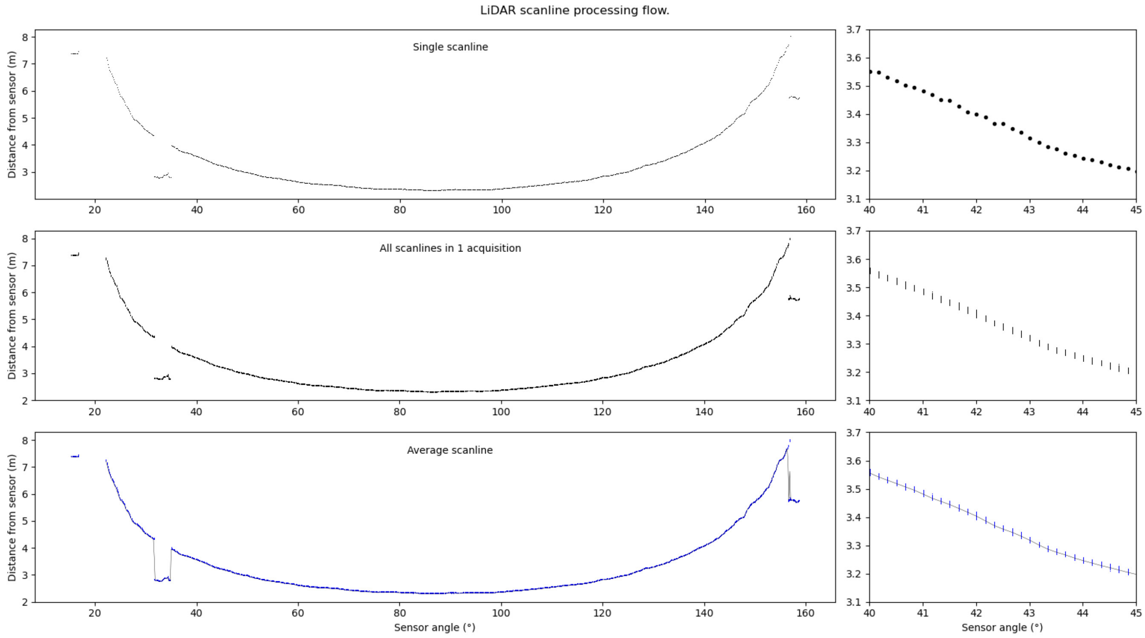

Figure 25 - Processing individual scanlines to an average scanline of a dry section (which acts as a reference). Top row: single scanline. Middle row: complete record of scanlines in 1 acquisition. Bottom row: average scanline calculated from the scanline set. Detail view shown in right column.

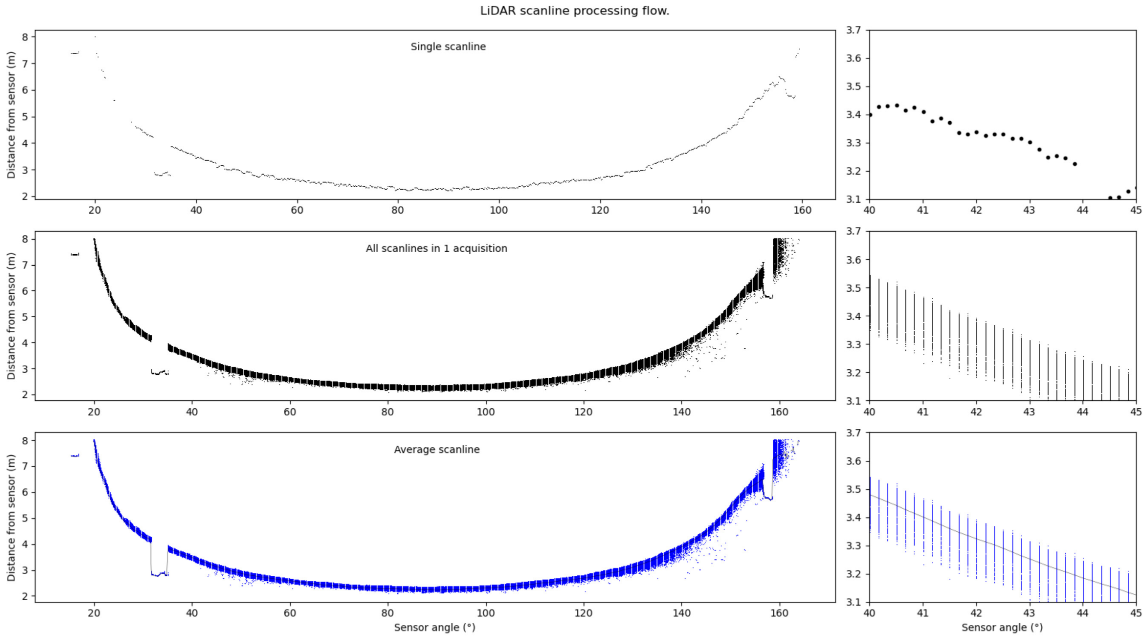

Figure 26 - Processing of individual scanlines of a scanline acquired during ongoing overflow.

On the images shown, the sensor portals over the test section are visible. Because these objects are assumed to be static in the field, the different records of a given section are aligned based on manually selected points corresponding to these small portals.

The alignment procedure is based on the minimization of the cloud-to-cloud distance of the selected points of each scanline. While performing the necessary transformation ((x,y)-translations and rotation), the final rotation is applied so that the toe or crest area is positioned

 This project has received funding from the Interreg 2 Seas programme 2014-2020 co-funded by the European Regional Development Fund under subsidy contract No [2S07-023]

horizontally[2]. After geometric reconstruction, the result obtained are presented in Figure 26. A cloud width of ca. 20 cm can be observed. Note that within a certain range, the measurements are reflected over a zone until the bottom level and even somewhat further. With an increase in angle between LiDAR and water surface, the measurements detach due to limited penetration of the LiDAR pulse. For the measurements on the crest, where the flow pattern isn't turbulent or foaming, the variation in reflected cloud thickness is limited. A concern is that within a certain angle with respect to the water surface the LiDAR beam seems to be partially reflected on the water surface, within the water column and on the bottom level (i.e. the levee slope), see Figure 26 lower right, this behavior may also vary with the incidence angle.

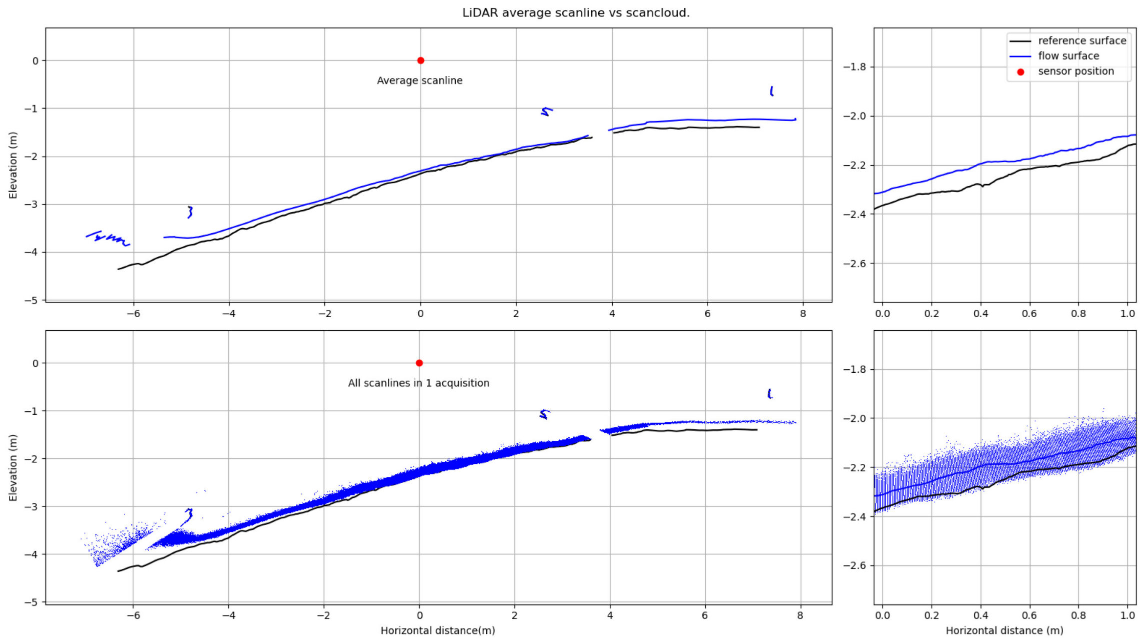

Figure 27 - View of a reference (black points) and a flow scan (blue) after alignment and horizontal restoration.

At the positions of the small sensor portals, a point is selected in order to calculate an average water depth at that position. There are two factors influencing the accuracy of the result. Firstly, the ultrasonic water level sensor is not located directly in the scanline position. Secondly, the ground reference is spatially irregular which makes a "true" depth impossible to identify. Therefore, it is acceptable that an area is selected over which the average water depth is identified. The x-position of the portals is (manually) selected, and the LiDAR surface data (excluding the portal datapoints) in a range of +/- 25 cm from the selected position are automatically selected. This yields several datapoints which will then be further analyzed.
The resulting water depths in the example shown above, are quantified as 18.6 cm for the lower portal and 4.5 cm for the upper portal. When looking at the pointcloud, one must realize that irregular surfaces, foaming and bubbling influence the results and that the given depth is an average. In order to obtain insight in this, the following statistics are calculated for each

[2] In future applications, the slope of the levee could be matched to the real slope if topographic measurements are available.

This project has received funding from the Interreg 2 Seas programme 2014-2020 co-funded by the European Regional Development Fund under subsidy contract No [2S07-023]

point: mean level of scan, p95 level of the scan (highest level) and a standard deviation. In Figure 27, the statistics for such a point are plotted together with the original data clouds as an example.

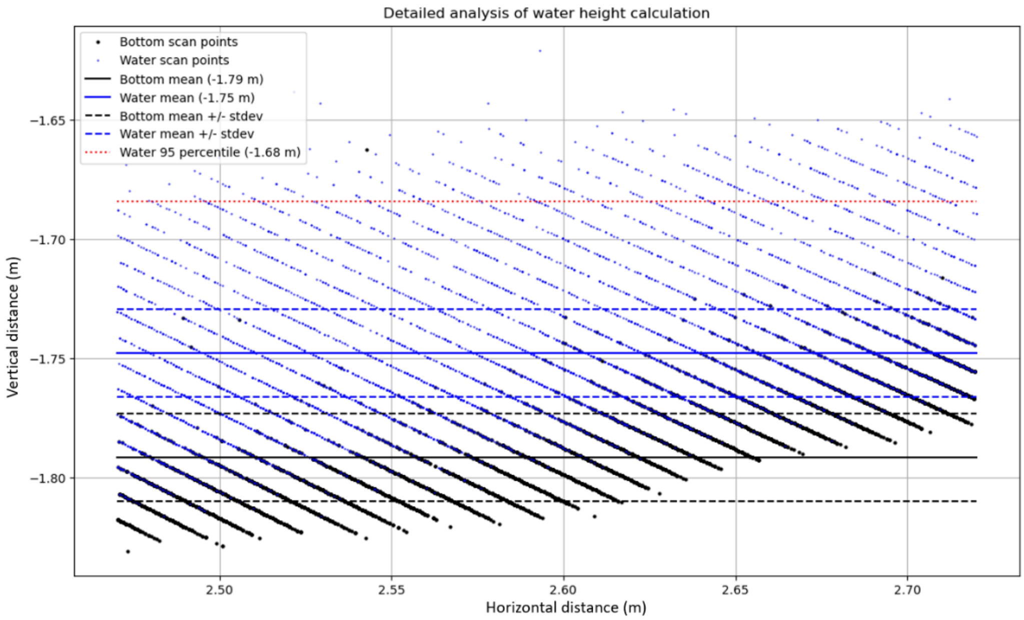

Figure 28 - Statistical analysis of scandata to yield a mean and 95-percental surface or water level position. The horizontal lines indicate the average levels within the 25 cm wide bin.

<u>Data selection</u>

The comparison of the two measurement types is performed at positions where reliable and sufficient data is available, especially when varying discharges were applied. The analyzed positions are:

- Overflow test B-OF08 block 11 UPPER position
- Overflow test B-OF10 block 11 UPPER position
- Overflow test B-OF11 block 12 UPPER position
- Overflow test N-OF03 block 6 UPPER position

3.2.3 Comparison

3.2.3.1 B-OF08 Block 12 (Upper position)

Data were acquired during Block 12 under varying flow conditions, ranging from Q=110 to 750 l/s, or q = 55 to 375 l/s.m. The position of the LiDAR scanner is on the upper camera portal (Figure 28). The LiDAR measurement encompasses the ultrasonic water level positions 'UPPER' and 'MOBILE'. The image shows the result for discharge Q = 200, 400 and 750 l/s. There is no valid 'MOBILE' comparison data. Therefore, this position is not further detailed in the analysis. The mean and p95 water level from the LiDAR are compared with the mean water height from the ultrasonic device in the UPPER position in Table 1, Figure 29 and Figure 30.
The observations statistics show fairly good correlations (R^2 ranging from 0.98 (Lidar mean depth vs Ultrasonic depth) to 0.98 (Lidar p99 depth vs Ultrasonic depth)) across a varying discharge. However, the actual values between the mean LiDAR and mean ultrasonic water height do not correspond very well. The correspondence between the p95-water height from

 This project has received funding from the Interreg 2 Seas programme 2014-2020 co-funded by the European Regional Development Fund under subsidy contract No [2S07-023]

the LiDAR cloud is much better than the mean point cloud depth (Table 1). This would suggest that the LiDAR scanner reflects 'deeper' in the water (and foam) layer than the ultrasonic sensor.

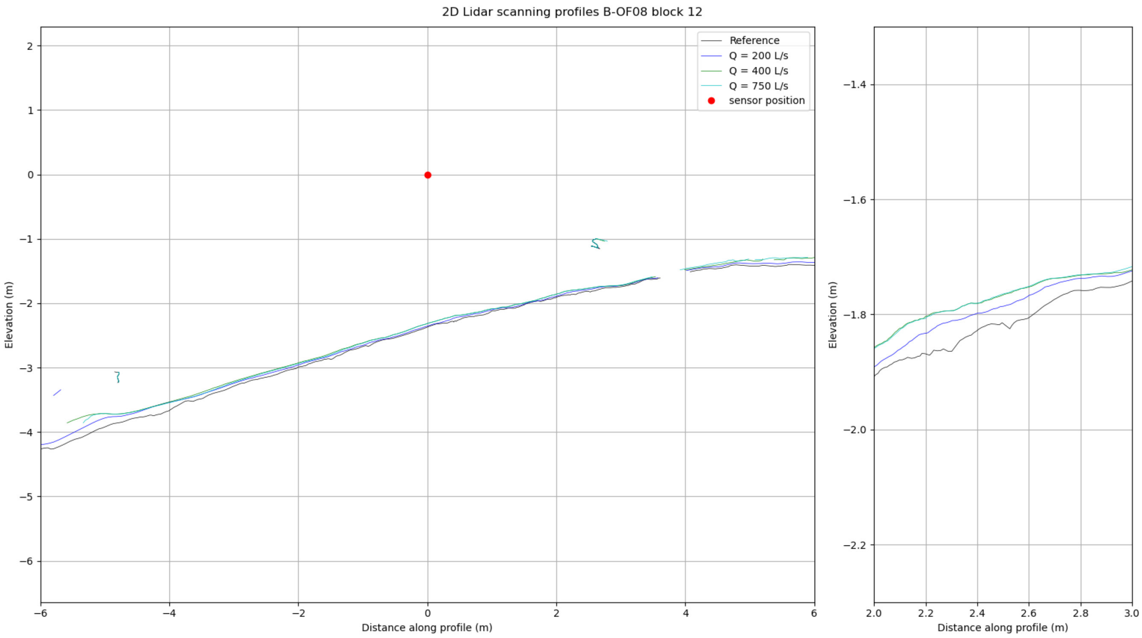

Figure 29 - Scan data from the B-OF08 Block 12 test at 3 distinct discharges and a dry reference.

Table 1 - Water height statistics based on B-OF08 Block 12 at the Upper sensor position, for different discharge regimes.

Nominal pump discharge (L/s)	Observed q (L/s/m)	Portal upper Water height (cm)		
Q	q	LiDAR mean	LiDAR p95	Ultrasonic
110	51.0	0.8	3.9	4.4
200	94.5	3.1	6.9	5.8
260	138.0	4.1	8	6.8
320	160.0	4.3	8.3	7.4
400	197.5	4.6	9.1	8.3
450	222.5	4.8	9.5	9
500	245.5	4.4	9.3	9.6
550	266.0	4.5	9.7	10
575	282.5	4.5	9.5	10.5
625	319.5	4.7	10.1	11.5
675	333.5	4.9	10.4	12.2
750	374.5	5.2	11.6	13.2

This project has received funding from the Interreg 2 Seas programme 2014-2020 co-funded by the European Regional Development Fund under subsidy contract No [2S07-023]

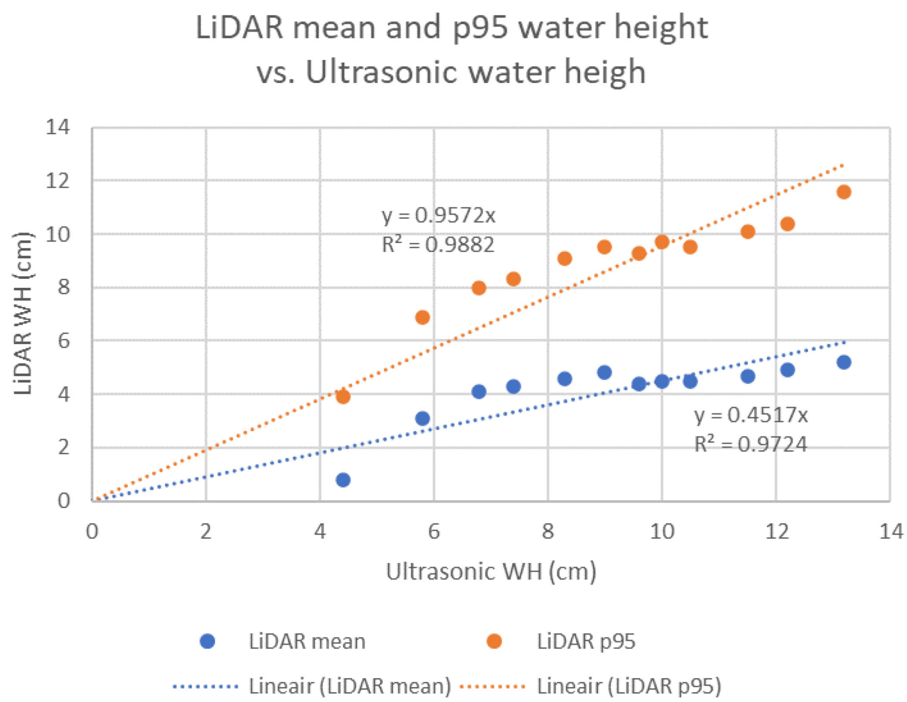

Figure 30 - Correlation of the LiDAR vs Ultrasonic based water height (based on different discharge regimes) (B-OF08 Upper position).

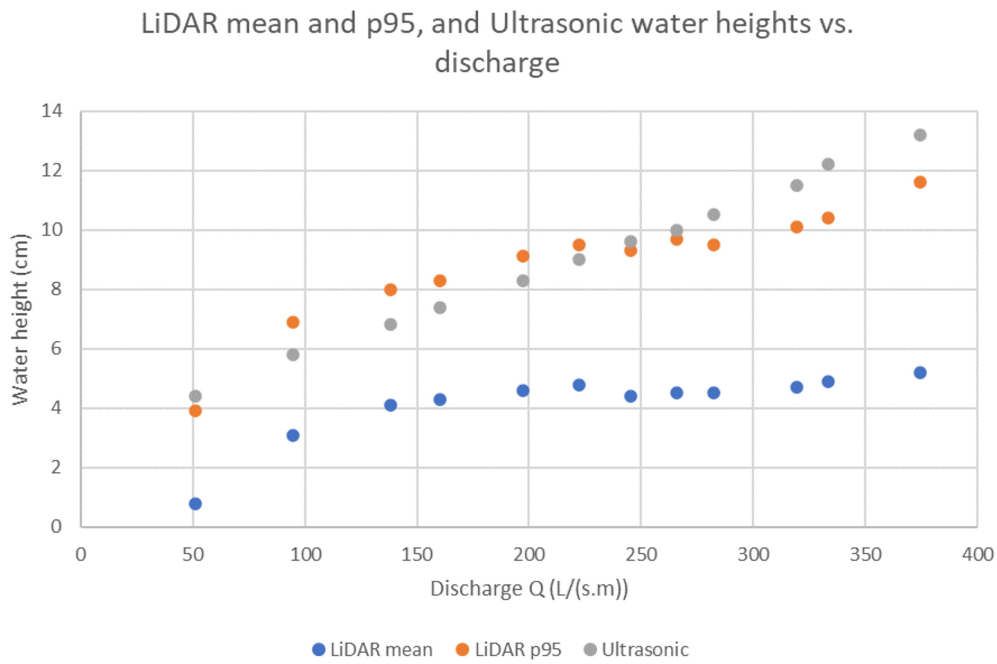

Figure 31 – Comparison of the LiDAR and Ultrasonic based water height (based on different discharge regimes) against the applied discharge (B-OF08 Upper position).

This project has received funding from the Interreg 2 Seas programme 2014-2020 co-funded by the European Regional Development Fund under subsidy contract No [2S07-023]

3.2.3.2 *B-OF10 Block 11*

During overflow test B-OF10, discharge variations were made in Block 11. Pump discharges applied were 80, 130, 220, 260 and 275 l/s. LiDAR scans were made during this run for each discharge scenario (Figure 31). For this section, both UPPER and MOBILE portal statistics can be compared (Table 2). In contrast to the results for B-OF08, the best correspondence between measurement values is achieved for the mean LiDAR scan statistic; although the correlation coefficients are higher for the p95 (0.88) than for the mean (0.77) height there is an offset between both; the actual values for the mean heights correspond better. Also, the p95 value seems to flatten out quickly. This observation stands for both the UPPER and MOBILE sensor location.

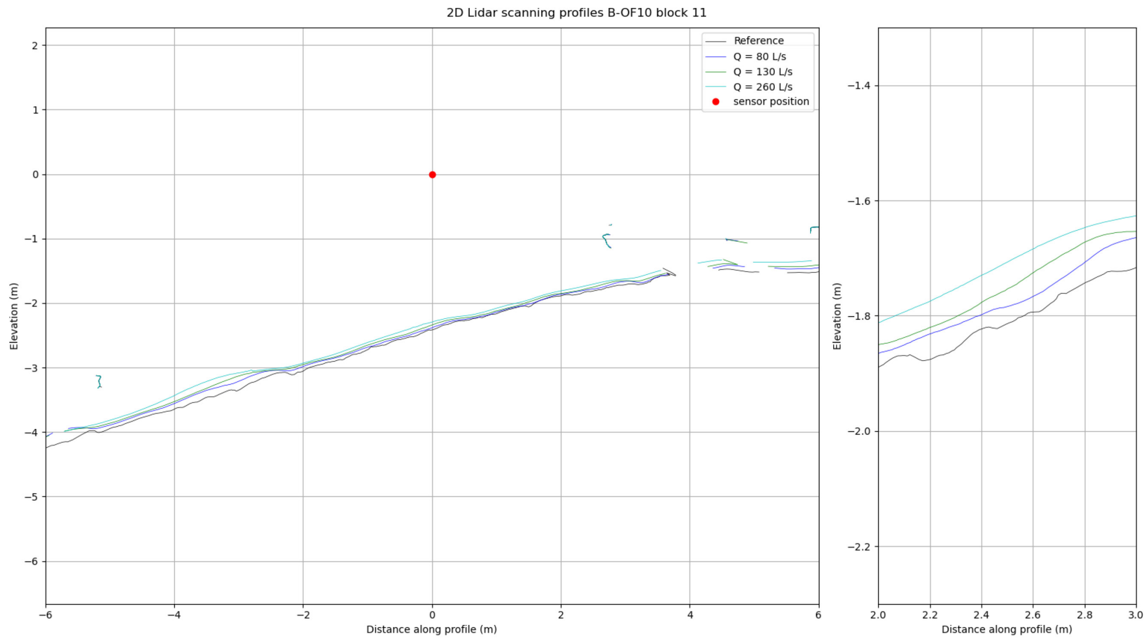

Figure 32 - Scan data from the B-OF08 Block 11 test at 3 distinct discharges and a dry reference. The Mobile sensor position is located at -5.5 m, the Upper at 2.5 m along the x-axis. The portal bars are visible in the reflections.

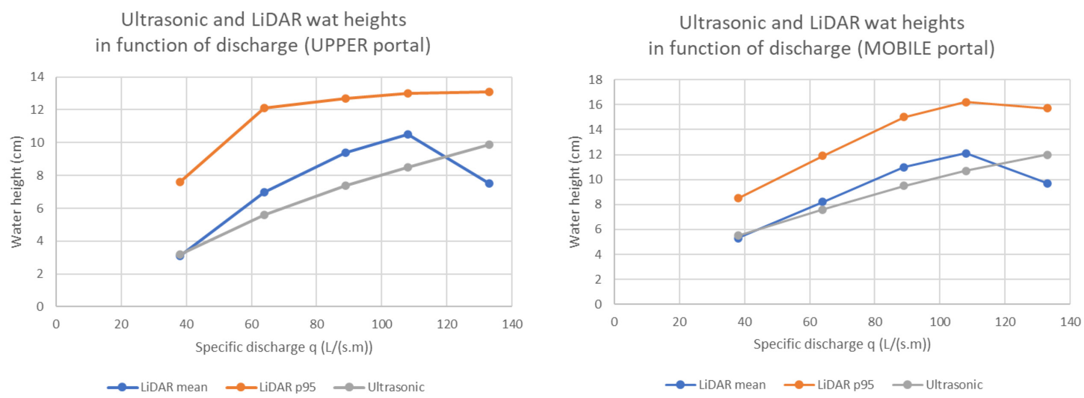

Figure 33 - Comparison of the LiDAR vs Ultrasonic based water height (based on different discharge regimes) for the UPPER and MOBILE portal.

This project has received funding from the Interreg 2 Seas programme 2014-2020 co-funded by the European Regional Development Fund under subsidy contract No [2S07-023]

Table 2 - Water height statistics based on B-OF10 Block 11 at the Upper sensor position, for different discharge regimes.

Nominal pump discharge (L/s)	Observed q (L/s.m)	Portal upper Water height (cm)			Portal mobile Water height (cm)		
	q	LiDAR mean	LiDAR p95	Ultrasonic	LiDAR mean	LiDAR p95	Ultrasonic
80	38	3.1	7.6	3.2	5.3	8.5	5.5
130	64	7.0	12.1	5.6	8.2	11.9	7.6
220	89	9.4	12.7	7.4	11.0	15.0	9.5
260	108	10.5	13.0	8.5	12.1	16.2	10.7
275	133	7.5	13.1	9.9	9.7	15.7	12.0

3.2.3.3 *B-OF11 Block 12*

During Block 12 of overflow test B-OF11, the following discharges were applied: 76, 104, 290 and 500 l/s. For the lowest discharges 76 and 104 l/s.m, the upper portal did not yield any reliable LiDAR data. For the higher discharges, results were obtained. From the data it follows that here too, the Ultrasonic corresponds better to the LiDAR mean (R^2=0.99) water height than to the LiDAR p95 (R^2=0.92) water height.

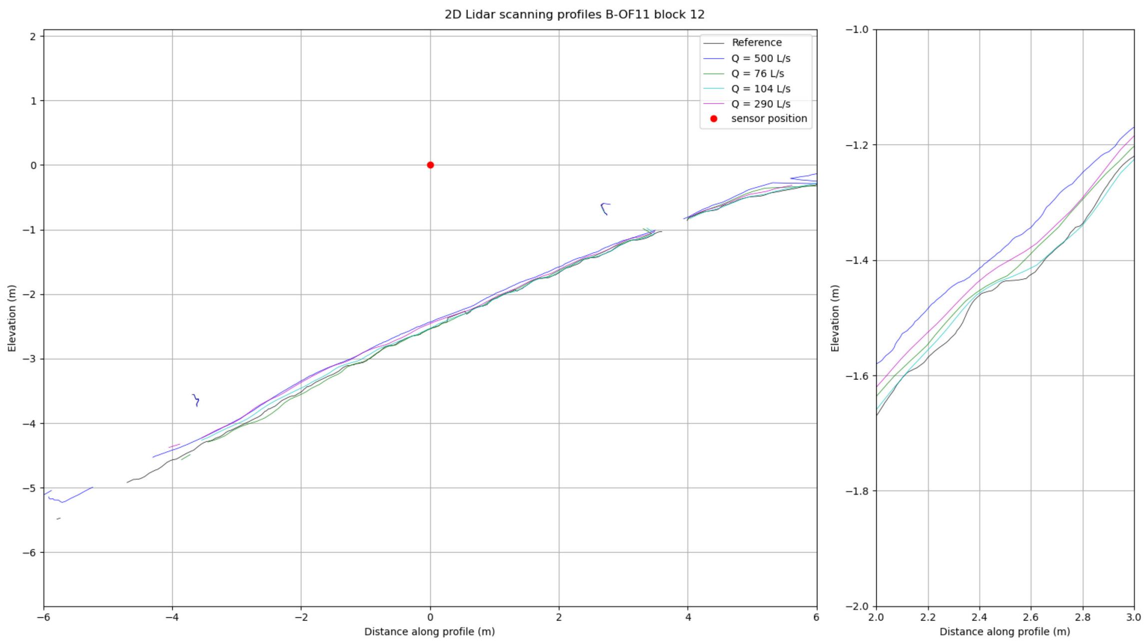

Figure 34 - Scan data from the B-OF11 Block 12 test at 3 distinct discharges and a dry reference.

This project has received funding from the Interreg 2 Seas programme 2014-2020 co-funded by the European Regional Development Fund under subsidy contract No [2S07-023]

Table 3 - Water height statistics based on B-OF11 Block 12 a the the Upper and Mobile sensor position, for different discharge regimes.

Nominal pump discharge (L/s)	Observed q (L/s)	Portal upper Water height (cm)			Portal mobile Water height (cm)		
	q	LiDAR mean	LiDAR p95	Ultrasonic	LiDAR mean	LiDAR p95	Ultrasonic
76	100	-	-	2.4	6.0	12.2	3.6
104	122	-	-	4.1	8.6	13.3	4.9
290	215	6.8	14.7	7.2	10.1	14.7	8.7
500	334	8.3	16.3	8.5	11.2	18.1	12.9

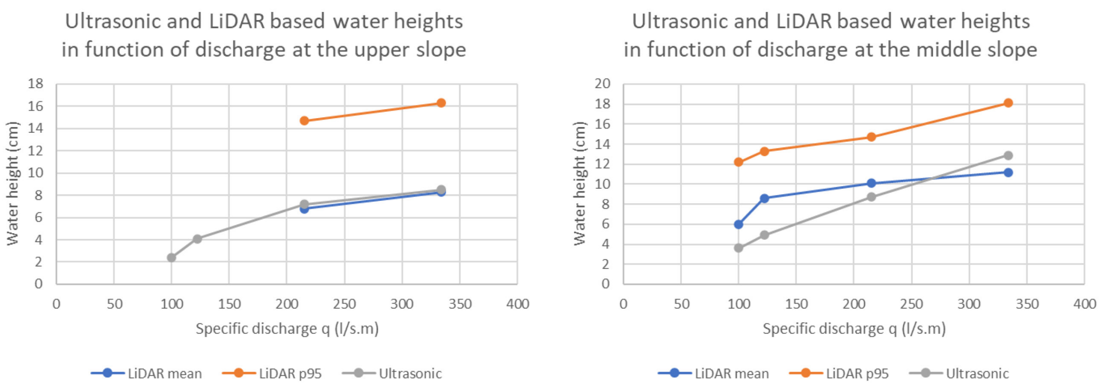

Figure 35 - Comparison of the LiDAR vs Ultrasonic based water height (based on different discharge regimes) for the Upper and Mobile portal.

3.2.3.4 N-OF03 Block 6

A complication for the full analysis of the monitoring timeseries of experiment N-OF03 is the lack of reliable discharge measurements. However the revolutions per minute (rpm) of the pump are mentioned in the logbook. Therefore, a discharge is not shown, just the pump power in RPM. A conversion formula from rpm to discharge is presented in §2.3. The three applied rpm's 1200,1400 ,1600 correspond with an estimated discharge of 320 L/s.m, 546 L/s.m and 772 L/s.m.

From what is observed on the upper and mobile water level sensor position, there is a fairly good correspondence between the ultrasonic measurement and the LiDAR p95 measurement at the Upper location. At the mobile position, the LiDAR mean depth equals the Ultrasonic mean value for the discharge corresponding with the pump power 1200 rpm. For the higher discharges the Ultrasonic measurement is in between the mean and the p95 value, slightly more towards the mean value.

This project has received funding from the Interreg 2 Seas programme 2014-2020 co-funded by the European Regional Development Fund under subsidy contract No [2S07-023]

Table 4 - Water height statistics based on N-OF03 Block 6 at the Upper and Mobile portal position.

Nominal pump discharge (rpm)	Portal upper Water height (cm)			Portal mobile Water height (cm)		
	LiDAR mean	**LiDAR p95**	**Ultrasonic**	**LiDAR mean**	**LiDAR p95**	**Ultrasonic**
1200	14.1	21.1	21.0	9.3	14.6	9.3
1400	17.9	24.9	24.5	10.4	15.8	12.4
1600	20.6	27.6	24.6	12.1	17.6	14.6

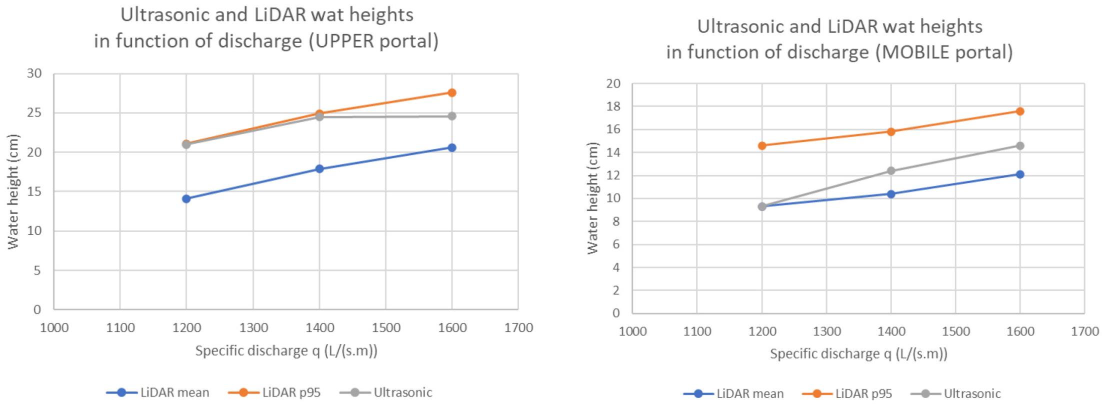

Figure 36 - Comparison of the LiDAR vs Ultrasonic based water height (based on different discharge regimes) for the Upper and Mobile portal.

3.2.4 Conclusion

Based on 4 sets of observations on 3 different overflow tests, the LiDAR based (mean) water level appeared to correspond to the Ultrasonic mean water level to a fair degree, although there is an important variation in the agreement:

- In the case of B-OF08, it appeared that the LiDAR p95 water level corresponds best to the Ultrasonic water level. With an intercept forced at (0,0), the relation was nearly 1:1 on average.
- In other cases (B-OF10, B-OF11) the LiDAR mean water level provided the best correspondence.
- For the N-OF03 test, the match depends on the position of the portal; i.e. the upper slope portal shows better agreement with the p95 value, and the middle slope portal with the mean value.

It can be expected that both sensor devices are sensitive to foam, bubbles and spray. Experiments in a controlled environment would be required in order to elucidate under which conditions one or the other method is more or less sensitive. The LiDAR measures a very small instantaneous spot, while the Ultrasonic samples a certain area. LiDAR measurements have a slanted view on the surface (depending on the angle of incidence), whereas the ultrasonics were mounted perpendicular to the flow direction. Both measurement devices only present

 This project has received funding from the Interreg 2 Seas programme 2014-2020 co-funded by the European Regional Development Fund under subsidy contract No [2S07-023]

one value and not the intensity of the reflection in time. Based on field trials, in challenging conditions, it is not conclusive to say which method is the best. Nevertheless, the apparent advantage of the LiDAR system is that 2D profiles of the water surface can be portrayed, whereas the Ultrasonic system seems to be very robust and yield timeseries with relatively small variability over time. In order to better understand the relative performance of both devices, it would be worth wile to investigate under conditions with more control on spray, bubbles and aeration in the water column.

3.3 Velocity

3.3.1 Methods

In this paragraph the velocity measured by the default three electromagnetic point flow velocity meters is compared with velocities derived from PTV and LSPIV measurements. The comparison of the point velocity measurements with PTV is carried out for section B-OF8 block 12 and the comparison of the point velocity meters with LSPIV measurements is carried out for section B-OF11 block 11 and block 12. The processing of the point velocity measurements, the LSPIV measurements and the PTV measurements is described in §2.5, §2.6 and §2.7. For the point velocity measurements the velocity vector is used for the comparison. The measurements used for comparison are presented in §3.3.2, the intercomparison is given in §3.3.3, conclusions are formulated in §3.3.4.

3.3.2 Data

For a comparison of the three point velocity meters with PTV measurements, OF8 block 12 is considered. During this block, PTV recordings were performed for 5 discharges ranging from approx. 60 l/s. m to approx. 380 l/s.m. The three point velocity meters (upper, mobile and lower) were on their default location, see Figure 23. Pre-processed timeseries of the point velocity measurements for OF8 Block 12 during the period of the PTV measurements are presented in Figure 36. Note that for the period with the lowest discharge the variance of the 1 s averaged signal increases significant expected the highest velocities are measured at location lower. The velocities measured at the location upper are higher than the velocity measured at the location mobile, situated in between.

This project has received funding from the Interreg 2 Seas programme 2014-2020 co-funded by the European Regional Development Fund under subsidy contract No [2S07-023]

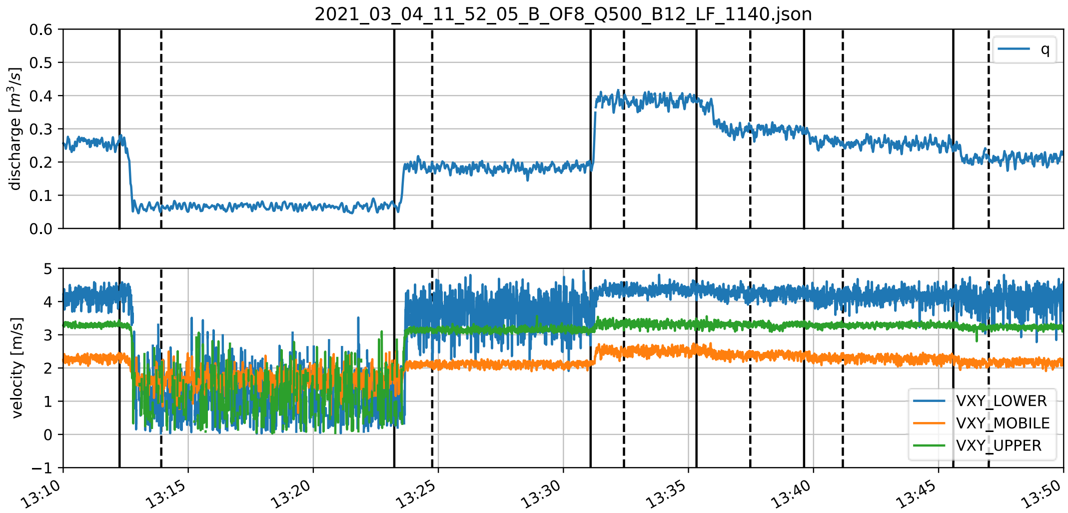

Figure 37 – Measured discharge and point velocity during B-OF8 block 12

A merged recording of the water surface during 4 overflow discharges is presented in Figure 37. Note that the upper and lower portal are visible. The mobile portal is located just at the gap in the middle and is therefore not visible. For the 4 presented discharges, the flow is non-aerated at location upper and aerated at location mobile and lower.

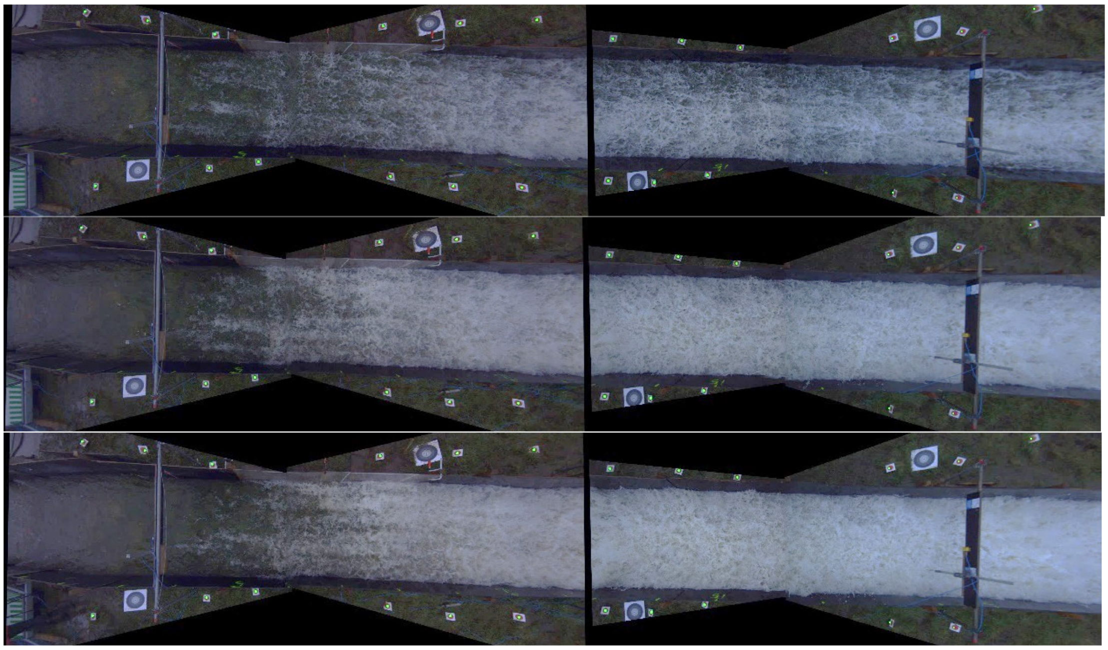

This project has received funding from the Interreg 2 Seas programme 2014-2020 co-funded by the European Regional Development Fund under subsidy contract No [2S07-023]

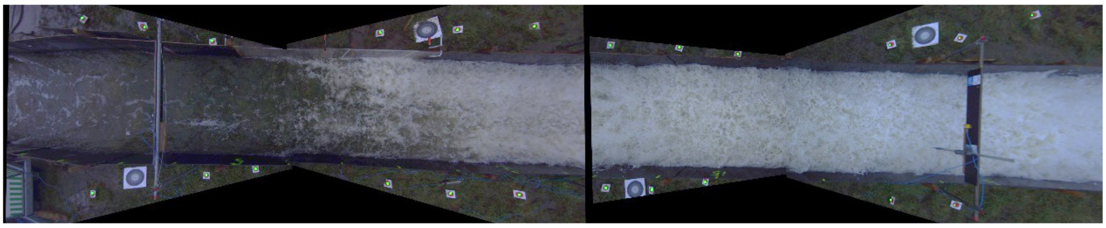

Figure 38 – B-OF8 block 12 recording
(from top till bottom q=85 L/s.m, q=175 L/s.m, q=300 L/s.m, q=375 L/s.m)

Figure 38 shows the results of the PTV measurements for B-OF8 block 12, the point to point velocity is presented in the upper panel and the three point moving average in the lower panel. The distance in between two consecutive measurement points at the slope is in between 0.2 m and 0.9 m depending on the location on the slope and the specific discharge. At some points the object becomes submerged and the following frame will be used, in this case the distance between the measurement points doubles or even triples. Note that the successive values can show some variation and that at approx. 11 m there is a discontinuity. A possible explanation for the discontinuity at 11 m is that the displacement is calculated between two different camera's. The three point moving average is more stable and will be used for further analysis. The measurement points closest to the locations of the upper, mobile and lower point velocity meter are considered for the comparison with the point velocity measurements.

The PTV measurement shows an increase in velocity on the landward levee slope. For the lowest discharge it seems that the equilibrium velocity is reached. For the higher discharges the velocity seems to evolve towards the equilibrium velocity. Based on a visual interpretation of the figures, it cannot be said whether it is also achieved. The results show an increase of velocity with discharge. However the largest increase is noticed between the lowest and second discharge while for a further increase in discharge the increase in velocity is less pronounced. Overall the PTV measurements are considered trustworthy. From the second lowest discharge (i.e. 350 l/s) the velocity on the slope reaches 5 m/s or higher exceeding the measurement range of the point velocity meters.

 This project has received funding from the Interreg 2 Seas programme 2014-2020 co-funded by the European Regional Development Fund under subsidy contract No [2S07-023]

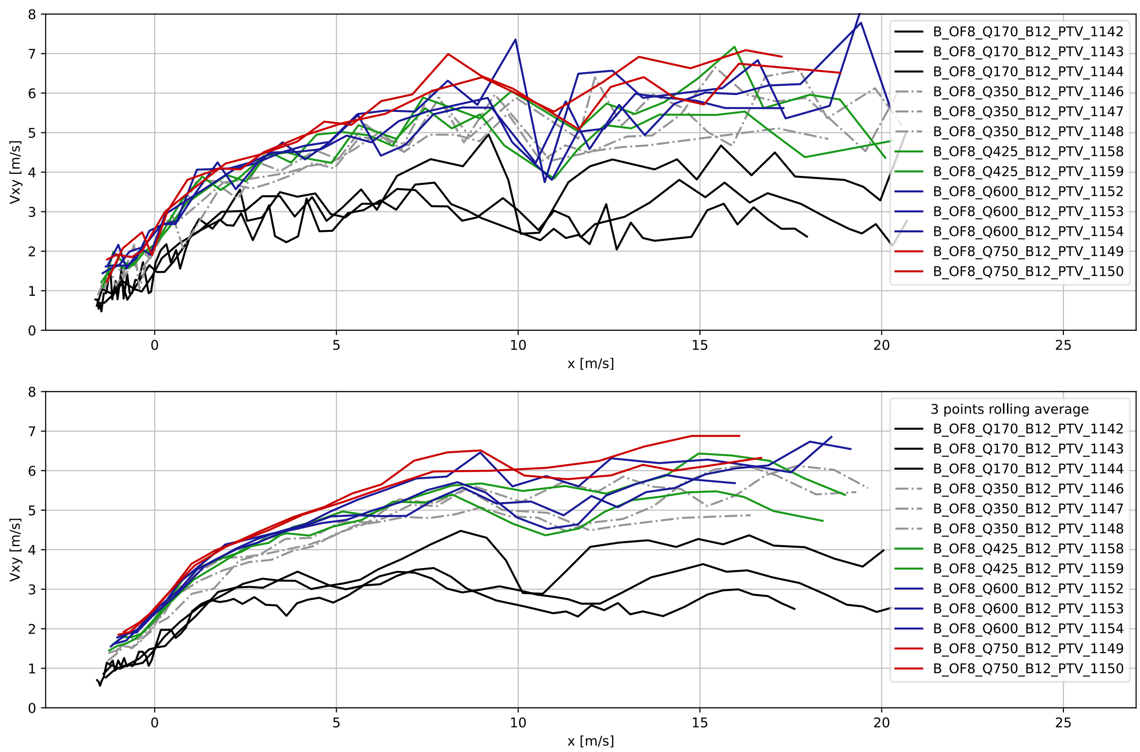

Figure 39 – B-OF8 block 12 results PTV measurements

For the comparison of the results obtained with the Valeports, i.e. the three point velocity measurement devices, with LSPIV measurements B-OF12 block 11 and block 12 are considered. During block 11 the LSPIV camera was mounted on the lower camera profile while during block 12 the LSPIV camera was mounted on the upper camera profile. Note that also during N-OF03 block 6 LSPIV measurements were performed. During this block only 2 Valeports were used, both located on the crest. For this reason the comparison is limited to B-OF12.

Pre-processed timeseries of the point velocity measurements for B-OF12 block 11 and block 12 during the period of the LPIV measurements are presented in Figure 39. Note that the transitions in velocity corresponds to a transition in discharge. It should be expected that the lowest point velocity is measured at the upper location, while at the lower location the velocity is higher or equal to the velocity at the location mobile. For the highest discharges the variance of the measured velocity on the location upper is limited but the variance increases with a decrease in discharge. Figure 40 illustrates that for the higher discharges the aeration starts downstream from location upper. The point velocity meter at location upper is measuring in non-aerated, accelerating but more or less steady flow condition. While at location mobile and location lower, the flow is aerated and much more turbulent. For block 11 during the highest discharge the velocity measured at the location lower is below the velocity measured at location upper what is not realistic. For the lowest discharge both during block 11 and block 12 the variance of the measurement at location mobile drops. A possible explanation could be lack of water depth. Maximum time averaged velocities till 4 m/s are measured, while the extremities in general stays below 5 m/s (i.e. the measurement range). When altering discharge the relationships between the three point velocity meters both in terms of mean and variance change in an illogical way.

This project has received funding from the Interreg 2 Seas programme 2014-2020 co-funded by the European Regional Development Fund under subsidy contract No [2S07-023]

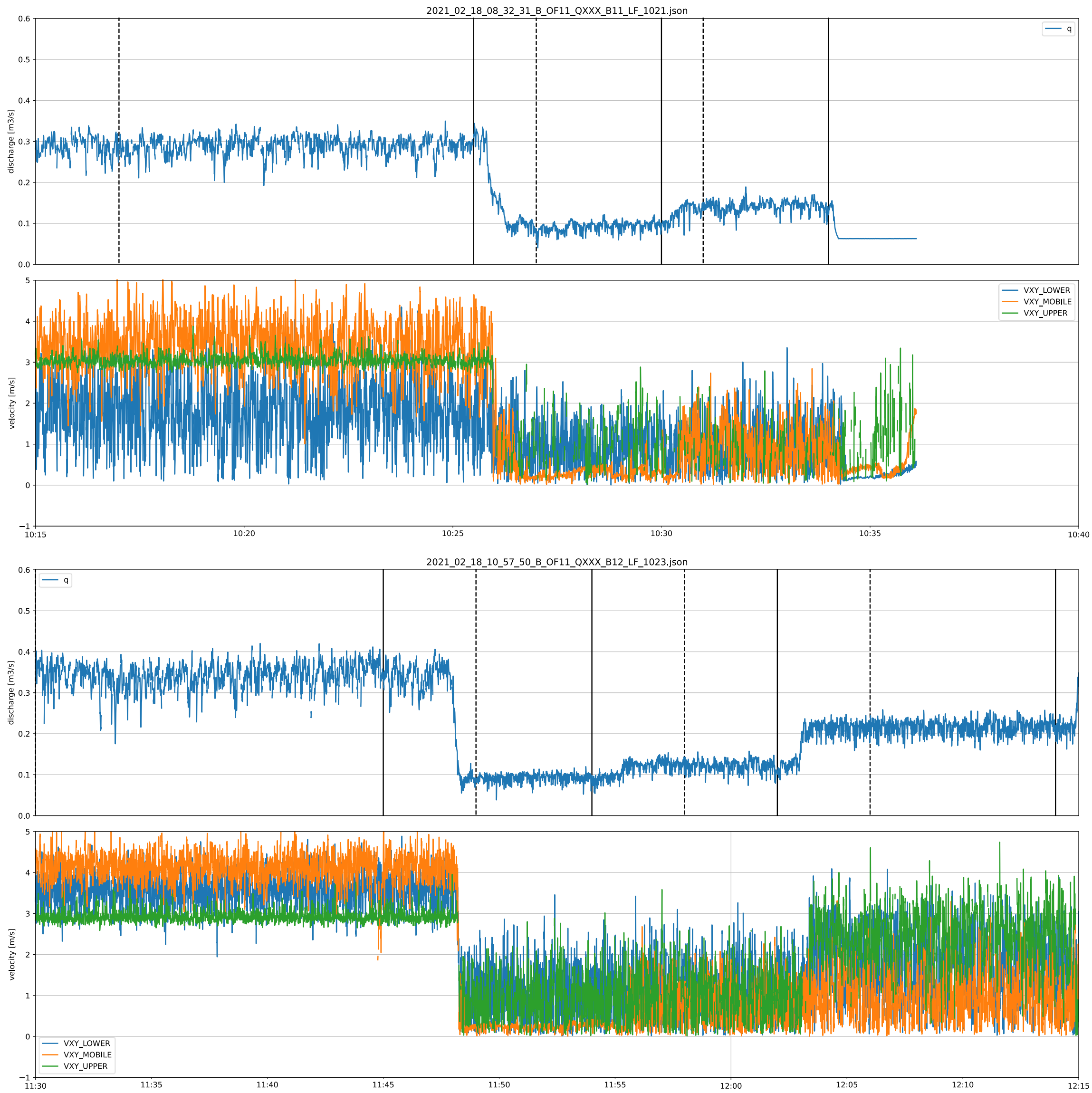

Figure 40 - Measured discharge and velocity (Valeport) during B-OF12 block 11(upper) and block 12 (lower)

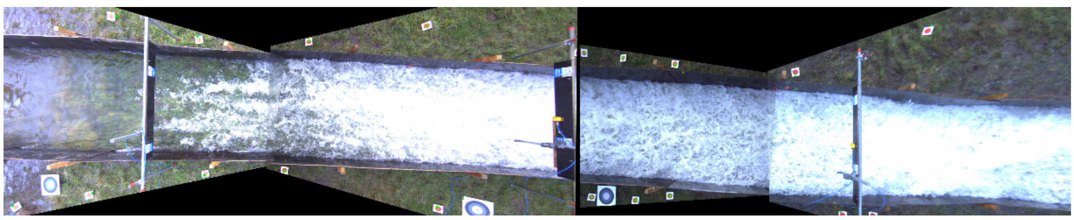

Figure 41 – Camera image during B-OF12 block 11 at 10:13 (q +/- 150 l/s.m)

Flow Velocities over section width derived from the LSPIV measurements during B-OF12 block 11 and block 12 are presented in Figure 41. During block 11 the LSPIV camera was mounted on the lower camera portal and during block 12 the LSPIV camera was mounted on the upper camera portal. The images are recorded at 160 fps. A visual check of the images reveals a clear shift of the overall image between two consecutive images. For each measurement 50 to 100 images were recorded and processed. The difference between the individual results and the averaged result was limited. In the direction of the flow

 This project has received funding from the Interreg 2 Seas programme 2014-2020 co-funded by the European Regional Development Fund under subsidy contract No [2S07-023]

the velocity was quite constant. Over the section width the results showed some variation. For this reason in Figure 41 the averaged velocity (over the images and the length along the flow direction) in function of the section width is presented. Note that for a given discharge the differences between the measurements are negligible. The LSPIV measurements of the surface velocity are considered trustworthy. At the lower portal, velocities up to 6m/s are obtained at the center during the highest discharge, thresholding the measurement range of the Valeports.

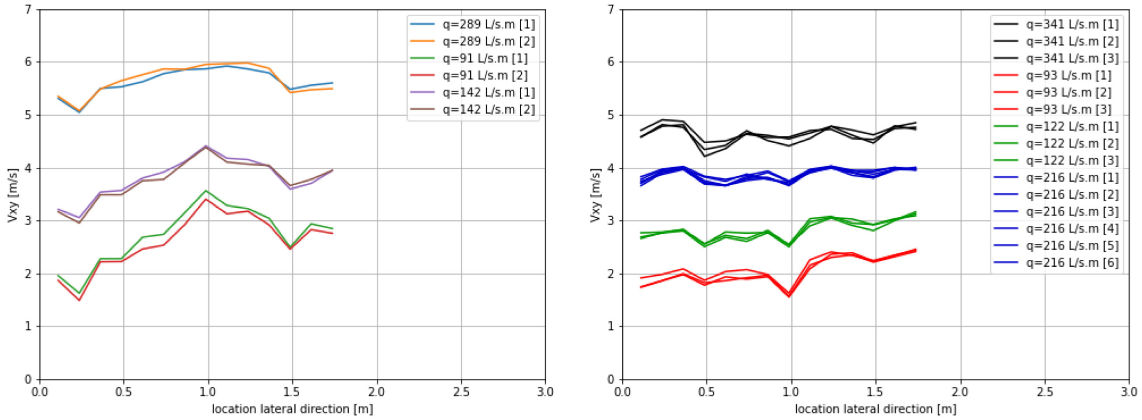

Figure 42 – Velocity over section width measured with LSPIV during B-OF12 block 11 (left) and block 12 (right)

3.3.3 Comparison

The comparison of the electromagnetic point velocity measurements with the PTV measurements is presented in Table 2. A graphical representation is given in Figure 42. In this figure also the section averaged velocity is presented, derived from dividing the specific discharge rate by the measured water height with the ultrasonic meters. Both the point velocity measurements as the PTV measurements show an increase of velocity with an increase in discharge for a certain location. For a given discharge the variance between the point velocity measurements is lower than 0.1 m/s, while for the PTV measurement the variance can be more than 1.5 m/s. For the lowest discharge the ratio of the electromagnetic point velocity meter to the PTV measurement at location upper and lower is notably higher. The presumable explanation is a lack of water depth for the point velocity meters during the lowest discharge. From a discharge 170 L/s.m on the ratio improves for locations upper and lower. For location upper the ratio is between 1.0 and 1.2, meaning that the velocity derived from the PTV is equal to 20% higher compared with the velocity measured by the point velocity meters. From the recordings follows that aeration starts downward from upper location. For location mobile the ratio increase till approximately 2.5, meaning that the velocity derived from the PTV is 2.5 times higher than the velocity measured by the point velocity meters. At location lower the ratio is between 1.1 and 1.7.

This project has received funding from the Interreg 2 Seas programme 2014-2020 co-funded by the European Regional Development Fund under subsidy contract No [2S07-023]

Table 5 – Comparison point velocity measurements (V_{EM}) with PTV – B-OF08 block 12

exp	Q	q	location								
			upper			mobile			lower		
	[l/s]	[l/s.m]	V_{EM} [m/s]	V_{PTV} [m/s]	V_{PTV} / V_{EM} [-]	V_{EM} [m/s]	V_{Ptv} [m/s]	V_{Ptv} / V_{EM} [-]	V_{EM} [m/s]	V_{PTV} [m/s]	V_{Ptv} / V_{EM} [-]
B_OF8_Q170_B12_PTV_1142	128	64	1.2	2.7	2.2	1.6	2.7	1.6	1.2	2.6	2.2
B_OF8_Q170_B12_PTV_1143	116	58	1.1	2.9	2.7	1.7	3.0	1.7	1.2	3.3	2.8
B_OF8_Q170_B12_PTV_1144	122	61	1.3	2.8	2.2	1.6	4.3	2.6	1.1	4.1	3.7
B_OF8_Q350_B12_PTV_1146	350	175	3.1	3.6	1.2	2.1	3.3	1.6	3.6	3.9	1.1
B_OF8_Q350_B12_PTV_1147	343	171	3.1	3.2	1.0	2.1	5.0	2.4	3.5	4.9	1.4
B_OF8_Q350_B12_PTV_1148	351	175	3.2	3.5	1.1	2.1	5.1	2.4	3.5	5.9	1.7
B_OF8_Q425_B12_PTV_1158	417	209	3.2	3.0	1.0	2.1	5.6	2.7	3.6	5.9	1.6
B_OF8_Q425_B12_PTV_1159	419	210	3.2	3.6	1.1	2.2	5.1	2.3	4.0	5.0	1.2
B_OF8_Q600_B12_PTV_1152	595	298	3.2	3.6	1.1	2.2	5.7	2.6	4.0	6.2	1.6
B_OF8_Q600_B12_PTV_1153	588	294	3.3	3.6	1.1	2.4	5.4	2.3	4.2	5.7	1.3
B_OF8_Q600_B12_PTV_1154	514	257	3.3	3.6	1.1	2.4	6.5	2.7	4.2	6.0	1.4
B_OF8_Q750_B12_PTV_1149	756	378	3.3	3.8	1.1	2.3	5.2	2.2	4.2	6.1	1.5
B_OF8_Q750_B12_PTV_1150	777	389	3.3	4.1	1.2	2.5	6.5	2.6	4.4	6.3	1.4

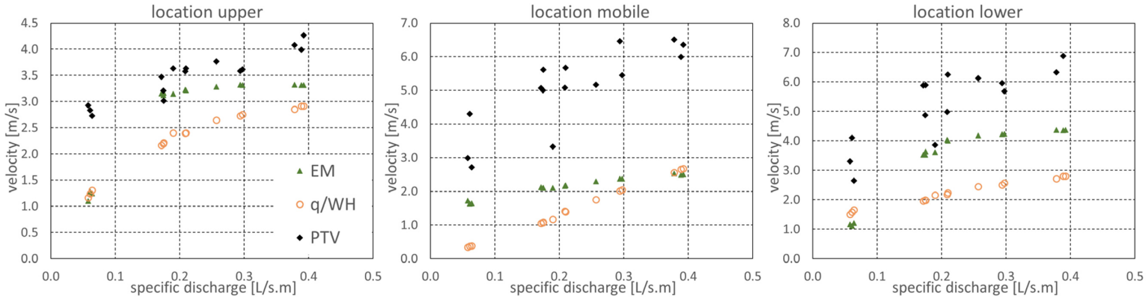

Figure 43 – Comparison of point velocity measurement (EM), section averaged velocity (q/WH) and particle tracking velocity for location upper (left), mobile (center) and lower (right)

From the comparison of the point velocity measurements with the PTV measurements following conclusions are drawn:

- At the lowest discharge of approx. 60 l/s.m the water depth is not sufficient for the point velocity meters.
- At location upper the velocity measured by PTV is 1.0 till 1.2 higher compared to the point velocity meter. Note that at location upper the velocity is below 5 m/s, the flow is not yet aerated and more or less steady. The point velocity meters are measuring within their design limits and the measured values are in range with the PTV measurement.
- At location mobile the velocity measured by PTV is approx. 2.5 times higher than measured by the point velocity meters. For B-OF8 block 12 the point velocity measured at location mobile is considered to be unreliable.

This project has received funding from the Interreg 2 Seas programme 2014-2020 co-funded by the European Regional Development Fund under subsidy contract No [2S07-023]

- At location lower the velocity measured by PTV is 1.1 to 1.7 times higher than the velocity measured by the point velocity meters. Possible explanations are capping of the measurement signal, aeriation of the flow and turbulence.

Note that the LSPIV images were recorded on a separated non-synchronized laptop with an observed shift in time. Therefore the comparison between the LSPIV measurements and the electromagnetic point velocity measurements was performed on time averaged values for a given discharge. The LSPIV measurements showed some variation in velocity over the section width. Unlike the PTV measurements, the LSPIV images are not referred to an absolute or local coordinate system. The exact location of the point velocity meters over the width was not registered. Therefore the averaged velocity (over the section width and over the separated measurements) is used for the comparison. The location of the LSPIV measurements was approx. 1.0 m upstream the camera portal. The LSPIV measurements are compared with the respective up- and downstream point velocity meter.

Table 6 - Comparison point velocity measurement (V_{EM}) with LSPIV (V_{LSPIV}) – B-OF11 block 11

q [L/s.m]	V_{EM} – location mobile x=9.4 m	V_{LSPIV} - location cam portal 2 x≈14.3	V_{EM} – location lower x=16.3 m
91	0.30	2.68	0.95
142	0.97	3.77	1.07
289	3.46	5.63	1.82

Table 7 - Comparison point velocity measurement (V_{EM}) with LSPIV (V_{LSPIV}) – B-OF11 block 12

q [L/s.m]	V_{EM} – location upper x = 2.4m	V_{LSPIV} – location cam portal 1 X ≈ 4.3 m	V_{EM} – location mobile X= 9.4 m
93	0.96	2.05	1.08
122	1.05	2.82	1.13
216	2.47	3.85	1.74
341	2.93	4.60	3.56

From the comparison of the electromagnetic point velocity measurements with the LSPIV measurements following conclusions are drawn:

- The point velocity measurements at location upper are consistently lower than the LSPIV measurements approx. 2 m downstream. Because the flow is expected to be accelerating at location upper this is logical.
- The point velocities measured at location mobile and lower are unrealistic low compared with the LSPIV measurements..

3.3.4 Conclusion

Both the LSPIV measurement of the water surface and the PTV measurements proved to be successful. The PTV measurements give an understanding in the development of the flow towards the equilibrium velocity. The added value of the LSPIV surface measurement is a local indication of the variation of the velocity over the section width. Extra insights could be gained by optical recordings through a transparent

 This project has received funding from the Interreg 2 Seas programme 2014-2020 co-funded by the European Regional Development Fund under subsidy contract No [2S07-023]

side boarding by a high speed camera. Due to difficulties with the battery and the challenging working conditions for a delicate high speed camera the quality of the recordings was lower than expected.

The default measurement set-up consisted of three electromagnetically flow meters at location upper, mobile (in between) and lower. The measurements were validated by the LSPIV and PTV measurements. The outcome was that at location upper, where flow was not yet aerated, the point velocity measurements and the PTV measurements gives a similar but 20 % different velocity. For the location mobile and location lower the point velocity measurement are not coherent and deviate with the PTV and LSPIV measured velocity. The explanation is presumable a combination of an exceeding of the measurement range of the electromagnetically flow velocity meters and the flow conditions at locations lower and mobile (highly aerated and turbulent).

It is concluded that only point velocity measurements taken at the crest or the portal position upper were the flow is still accelerating in not aerated flow are reliable. The point velocities measured at the location mobile and lower will most likely be an underestimation of the actual value.

This project has received funding from the Interreg 2 Seas programme 2014-2020 co-funded by the European Regional Development Fund under subsidy contract No [2S07-023]

4 Lessons learned

This report provides an overview of default and additional hydraulic measurements during the design and application of the overflow generator within the framework of the Interreg Polder2c project. Flanders Hydraulics was in the lead of the execution of the overflow tests. An overflow generator with the adjoining measurement set-up was developed for the overflow tests. The set-up was inspired by previous overflow tests performed by Infram and Inrae. Flanders Hydraulics has a vast experience in the development of indoor test and measurement set-ups. For the overflow tests the experience from indoor was taken outside.

The overflow generator itself proved to be well functioning both from a constructive as from a hydraulically point of view. More specific the material of the generator, High Density Polyethylene, proved optimal. The decision to work with a pressurized inlet connected to a dissipation box can be reconsidered for an adjusted design. The pomp set-up of the third test period proved to be much more flexible, a disadvantage was that the feeder lines were ending above the water surface within the overflow generator, resulting in a disturbed outflow of the generator. Note that an hydraulic well designed system with filling form the top would have led to an increase in dimensions. To have less difficulties with levelling of the generator, It can be considered to position the outflow of the generator below crest level. This will result in an increase in height of the overflow generator.

As part of the generator, a Data Acquisition System was developed to log the measurement data and a camera set-up with 4 camera's was used. Both the Data Acquisition System as the Camera set-up proved to be reliable, with respect to the used measurement devices. It should be noted that the clamp on ultrasonic discharge meter was not always reliable. Because discharge is the main parameter, this is a priority for improvement and a second alternative discharge measurement is recommended. The ultrasonic water height measurement proved to be consistent and reliable. To improve the hydraulic insights a thorough validation with a second technique with a higher frequency and reduced measurement spot is recommended. The electromagnetic point velocity meters proved to be unreliable in highly turbulent and aerated flow conditions and are therefore recommended not to be used in these circumstances. As a result, only at crest and before aeration of the flow, valid point velocity measurements were performed. The PTV measurements and the LSPIV water surface measurement were successful. With the PTV set-up the building-up of the velocity along the slope towards the equilibrium velocity is captured. With the LSPIV measurement variations of the flow velocity over the channel width are measured. The 2d LiDAR proved to be a valuable tool because both the bottom as the water surface are measured. Further (indoor) validation of the 2D LiDAR is needed. It's noticed within a certain range, even if the flow is expected to be aerated, that the LiDAR penetrates through the surface and is reflected somewhere in the water column and/or near bottom. With an increase in angle the accuracy is expected to decrease and also the risk of shadows in the measurement signal increases.

To conclude. Some lessons learned can be drawn mainly regarding the efficiency and measurement techniques. Overall it is concluded that the design, development and implementation of the overflow generator within the framework of the P2c project was successful.

This project has received funding from the Interreg 2 Seas programme 2014-2020 co-funded by the European Regional Development Fund under subsidy contract No [2S07-023]

5 References

Bonelli, S.; Nicaise, S.; Charrier, G.; Chaouch, N.; Byron, F.; Grémeaux, Y. (2018). Quantifying the erosion resistance of dikes with the overflowing simulator. *3rd Int. Conf. Prot. against Overtopping 6460*(*June*): 6–8
Depreiter, D.; Peeters, P.; Vercruysse, J.; Verelst, K.; Zomer, W.; Koelewijn, A.; Tsimopoulou, V. (2022a). P2c Summary report overflow and overtopping tests [CONCEPT]
Depreiter, D.; Vercruysse, J.; Verelst, K.; Zomer, W.; Koelewijn, A.; Tsimopoulou, V.; Peeters, P. (2022b). P2c Facutal data report - overflow tests on Belgian levees [CONCEPT]
Depreiter, D.; Vercruysse, J.; Verelst, K.; Zomer, W.; Koelewijn, A.; Tsimopoulou, V.; Peeters, P. (2022c). P2c Facutal data report - overflow tests on Dutch levees [CONCEPT]
Depreiter, D.; Zomer, W.; Van Dijck, P. (2022d). Comparison of handheld and topographic LiDAR measurements in the field. [CONCEPT]

Annex A - **Data format**

The measurement data captured by the data acquisition system was saved in the National Instruments TDMS file format. The analogue signals were convert to physical values by means of linear regression, characterized by an Acall and a Bcall factor. The used Acall, and Bcall factor for each channel are stored as meta data within the TDMS file format..

The tdms files are loaded by a python script by means of the .nptdms library. The water heights measurements are proceeded by 'WH' and expressed in m. The velocity measurements are proceeded by 'VX', 'VY' or 'VXT' and are expressed in m/s. VX the velocity along the flow axis, VY the velocity transversal to the flow axis and VXY the overall velocity. Note that the locations crest, upper, mobile and lower refer to the standard measurement set-up. During some measurement the sensors were repositioned. The exact locations of the sensors for a given test should be derived from the factual data report. For the preprocessed data in .json format following preprocessing is carried out:

- the height's and discharges are zeroed by means of the short period before starting the pump.
- the time series were despiked as explained by §3.2.2 for the water heights sensors and by §3.3.2 for the velocity sensors.
- Addition of following secondary values:
  - q Discharge per m width ($Q / W_{section}$) [m3/s.m]
  - H_{krit} Critical water height $h_c = (q^2/g)^{(1/3)}$ v$h_c = \sqrt[3]{\frac{q^2}{g}}$ [m]
  - H_{opw} Theoretical height river level $H_{river} = (q/C_d)^{(1/1.5)}$ [m]
- Adding of the time axis based on the moment of start recoding and the measurement frequency derived from meta data in the TDMS file. Note that the TDMS file format doesn't not contain a time axis. The time axis is presented in UTC+1.

Also a comma separated .csv file was prepared. The csv file was set-up starting from the json file with preprocessed data. The measurement period is increased from 0.1 s for the json to 1.0 s for the .csv file. The reduction was based on a moving average over a period of -0.5 s till +0.5 s.

 This project has received funding from the Interreg 2 Seas programme 2014-2020 co-funded by the European Regional Development Fund under subsidy contract No [2S07-023]